

Algebraic Phase Unwrapping Based on Two-Dimensional Spline Smoothing Over Triangles

Daichi Kitahara, *Student Member, IEEE*, and Isao Yamada, *Fellow, IEEE*

Abstract—Two-dimensional (2D) phase unwrapping is an estimation problem of a continuous phase function, over a 2D domain, from its wrapped samples. In this paper, we propose a novel approach for high-resolution 2D phase unwrapping. In the first step—Spline Smoothing (SPS), we construct a pair of the smoothest spline functions which minimize the energies of their local changes while interpolating, respectively, the cosine and the sine of given wrapped samples. If these functions have no common zero over the domain, the proposed estimate of the continuous phase function can be obtained by algebraic phase unwrapping in the second step—Algebraic Phase Unwrapping (APU). To avoid the occurrence of common zeros in SPS due to phase noise in the observed wrapped samples, we also propose a denoising step—Denoising by Selective Smoothing (DSS)—as preprocessing, which selectively smooths unreliable wrapped samples by using convex optimization. The smoothness of the proposed unwrapped phase function is guaranteed globally over the domain without losing any desired consistency with all reliable wrapped samples. Numerical experiments for terrain height estimation demonstrate the effectiveness of the proposed 2D phase unwrapping scheme.

Index Terms—Algebraic phase unwrapping, bivariate spline function, convex optimization, interferometric synthetic aperture radar, signal denoising, spline smoothing, terrain height estimation, two-dimensional phase unwrapping.

I. INTRODUCTION

TWO-DIMENSIONAL (2D) phase unwrapping [1], [2] is an estimation problem of an unknown continuous phase function $\Theta : \Omega \rightarrow \mathbb{R}$ from its noisy wrapped samples

$$\Theta^W(x, y) := W(\Theta(x, y) + \nu(x, y)) \in (-\pi, \pi] \quad ((x, y) \in \mathcal{G}), \quad (1)$$

where $\Omega (\subset \mathbb{R}^2)$ is a simply connected closed region, $\mathcal{G} (\subset \Omega)$ is the set of finite sampling points, ν is additive phase noise, and $W : \mathbb{R} \rightarrow (-\pi, \pi]$ is the *wrapping operator* defined by

$$\forall \vartheta \in \mathbb{R} \exists \eta \in \mathbb{Z} \quad \vartheta = W(\vartheta) + 2\pi\eta \text{ and } W(\vartheta) \in (-\pi, \pi].$$

Θ and Θ^W are called the *unwrapped phase* and the *wrapped phase* respectively. 2D phase unwrapping is important for signal and image processing applications such as *terrain height*

estimation (see Section IV-A) and *landslide identification* by interferometric synthetic aperture radar (InSAR) [3]–[9], *seafloor depth estimation* by interferometric synthetic aperture sonar (InSAS) [10]–[13], *3D shape measurement* by fringe projection [14]–[17] or X-ray [18]–[21], and *water/fat separation* in magnetic resonance imaging (MRI) [22]–[25].

As remarked clearly in [26], all commonly used phase unwrapping algorithms are based on the assumption that the true unwrapped phase field varies slowly enough that in most places, neighboring phase values are within one-half cycle (π rad) of one another, i.e., it is assumed that $\Delta\Theta_i := \Theta(\tilde{x}, \tilde{y}) - \Theta(x, y) \in (-\pi, \pi]$ for most neighboring pairs of samples $i := ((x, y), (\tilde{x}, \tilde{y})) \in \mathcal{G} \times \mathcal{G}$. Such algorithms have been designed to suppress a certain function J measuring the unwrapped phase differences $\Delta\Theta_i$ for all neighboring pairs $i \in \mathcal{G} \times \mathcal{G}$ as

$$J(\Theta) := \sum_i J_i(\Delta\Theta_i) \quad (\Theta := \text{vec}(\Theta(x, y))_{(x, y) \in \mathcal{G}}), \quad (2)$$

where $J_i : \mathbb{R} \rightarrow \mathbb{R}_+$ usually achieves 0 if $\Delta\Theta_i = W(\Delta\Theta_i^W)$, $\Delta\Theta_i^W := \Theta^W(\tilde{x}, \tilde{y}) - \Theta^W(x, y)$ is the wrapped phase difference between a neighboring pair $i = ((x, y), (\tilde{x}, \tilde{y}))$, and vec stands for the vectorization of multidimensional arrays. Such a specification of J_i is introduced on the basis of a simple property that, under the assumption $\nu = 0$,

$$\Delta\Theta_i = W(\Delta\Theta_i^W) \Leftrightarrow \Delta\Theta_i \in (-\pi, \pi]. \quad (3)$$

Then the algorithms try to use a minimizer of J as an estimate of the unwrapped phase.

Existing algorithms can be classified into two types. Major algorithms, [5], [25]–[30] assume that noise ν in (1) is small enough and try to find a minimizer of J under the condition

$$\forall (x, y) \in \mathcal{G} \exists \eta(x, y) \in \mathbb{Z} \quad \Theta(x, y) = \Theta^W(x, y) + 2\pi\eta(x, y). \quad (4)$$

This type of optimization problem is combinatorial and intractable due to condition (4). Therefore the algorithms first detect every closed loop having a *residue*¹ (see Fig. 12(a) in Appendix A). After identifying the residues, the algorithms construct the set of *branches* \mathcal{B} by connecting the positive and negative residues (see Fig. 12(b) in Appendix A). By defining E as the set of indices for neighboring pairs of samples which lie on either side of some branch in \mathcal{B} and by summing up continuously $W(\Delta\Theta_i^W)$ ($i \notin E$), we can construct a candidate of the unwrapped phase $\Theta(E)$ satisfying condition (4),

¹Note that this residue in 2D phase unwrapping is defined with a discretized contour integral for the wrapped phase over sampling points [1], [5] and different from the well-known *residue* in complex analysis.

Manuscript received February 22, 2015; revised August 06, 2015, October 21, 2015, and November 24, 2015; accepted December 03, 2015. Date of publication December 22, 2015; date of current version March 08, 2016. The associate editor coordinating the review of this manuscript and approving it for publication was Dr. Romain Couillet. This work was supported in part by JSPS Grants-in-Aid (26-920) and (B-15H02752).

The authors are with the Department of Communications and Computer Engineering, Tokyo Institute of Technology, Tokyo 152-8550, Japan (e-mail: kitahara@sp.ce.titech.ac.jp; isao@sp.ce.titech.ac.jp).

Color versions of one or more of the figures in this paper are available online at <http://ieeexplore.ieee.org>.

Digital Object Identifier 10.1109/TSP.2015.2510986

$\Delta\Theta_i(E) = W(\Delta\Theta_i^W)$ if $i \notin E$, and $\Delta\Theta_i(E) \neq W(\Delta\Theta_i^W)$ if $i \in E$ (see, e.g., [5], [25]–[30] and Fig. 12(b)). As a result, the cost in (2) is redefined as a function of E by

$$\hat{J}(E) := J(\Theta(E)) = \sum_{i \notin E} J_i(W(\Delta\Theta_i^W)) + \sum_{i \in E} J_i(\Delta\Theta_i(E)), \quad (5)$$

and the algorithms search for a minimizer E^* (or equivalently optimal branches \mathcal{B}^*) of \hat{J} to obtain an estimate $\Theta(E^*)$ (see Appendices A-(I) and A-(II)). In this paper, we call algorithms of this type *network flow methods* along [2], [26] because some of these algorithms use a technique developed originally for network flow in graph theory (see, e.g., Appendix A-(II)). In this approach, if the observed wrapped phase has only small noise and the true unwrapped phase differences are sufficiently small with respect to sampling interval, we can find E^* and construct a very good estimate $\Theta(E^*)$. However, otherwise, condition (4) is violated due to phase noise ν , and the minimizer E^* is hard to compute because the number of residues becomes large.

The other type of algorithms [24], [31]–[34], directly approximate a minimizer $\Theta^* = \text{vec}(\Theta^*(x, y))_{(x, y) \in \mathcal{G}}$ of J without requiring condition (4). In this approach, if the cost J is a certain convex function, we can find Θ^* and the computation time depends mainly on the size of Θ (see Appendix A-(III)). Therefore even if the observed wrapped phase is noisy and has many residues, Θ^* is obtained without suffering from the increase of the computation time. However since condition (4) is not required in the optimization problem, the consistency between Θ^* and Θ^W , i.e., $W(\Theta^*(x, y)) \approx \Theta^W(x, y)$, is not guaranteed at many sampling points $(x, y) \in \mathcal{G}$.

In this paper, we propose a completely different algebraic approach to 2D phase unwrapping by exploiting the property of $\Theta^W \in (-\pi, \pi]$:

$$\begin{aligned} \Theta^W &= W(\Theta + \nu) \\ \Leftrightarrow (\cos \Theta^W, \sin \Theta^W) &= (\cos(\Theta + \nu), \sin(\Theta + \nu)). \end{aligned} \quad (6)$$

The proposed scheme achieves a high-resolution estimate of the unwrapped phase Θ unlike many existing algorithms [5], [24]–[34]. We estimate Θ as the continuous phase function $\theta_f \in C^2(\Omega)$ of a twice continuously differentiable complex function $f := f_{(0)} + \nu f_{(1)} = |f|e^{i\theta_f}$, where $f_{(0)} \in C^2(\Omega)$ and $f_{(1)} \in C^2(\Omega)$ have no common zero over Ω (see Notation in the end of this section). Then the estimation problem of Θ is replaced with those of $f_{(0)}$ and $f_{(1)}$ which respectively approximate $\cos \Theta$ and $\sin \Theta$. Clearly, by (6), $f_{(0)}$ and $f_{(1)}$ are desired to interpolate $\cos(\Theta^W(x, y)) = \cos(\Theta(x, y))$ and $\sin(\Theta^W(x, y)) = \sin(\Theta(x, y))$ respectively if $\nu(x, y) = 0$ at $(x, y) \in \mathcal{G}$. Motivated by the main idea of *functional data analysis* [35]–[37], we assume that f is “smooth” which means that the energy of local change is small over Ω , and adopt the *bivariate spline space* as the set of all candidates of $f_{(0)}$ and $f_{(1)}$. After finding the smoothest spline functions $f_{(0)}^*$ and $f_{(1)}^*$ which are consistent with the wrapped phase information $\cos(\Theta^W(x, y))$ and $\sin(\Theta^W(x, y))$ at $(x, y) \in \mathcal{G}$ (*Spline Smoothing (SPS)*), the continuous phase function θ_{f^*} of $f^* := f_{(0)}^* + \nu f_{(1)}^* = |f^*|e^{i\theta_{f^*}}$ is analytically computed, as the proposed estimate of Θ , by *Algebraic Phase Unwrapping*

(APU) [38]–[42]. This approach has been proven particularly effective in the case where phase noise ν is relatively small and f^* has no zero over Ω . Indeed, by this approach, we can maximize a certain smoothness of θ_{f^*} subject to the condition $W(\theta_{f^*}(x, y)) \approx \Theta^W(x, y)$ for all sampling points $(x, y) \in \mathcal{G}$ (see Fig. 3 in Section III) unlike other algorithms.

Meanwhile, a central reason of the difficulty in 2D phase unwrapping has been due to the appearance of residues which are often caused by phase noise observed at even small portion of sampling points. Indeed, excessive fidelity to noisy wrapped samples erroneously influences the global feature of the results of existing 2D phase unwrapping algorithms (see, e.g., [1], [2], [43]–[45]). Such erroneous global features can also happen in the above proposed scheme (SPS and APU) as the path dependency of θ_{f^*} in APU due to the occurrence of zeros of f^* in SPS (see Fig. 4 in Section III). To suppress the influence of noise, we denoise, as a preprocessing step (*Denoising by Selective Smoothing (DSS)*), the wrapped phase Θ^W and obtain smoothed wrapped samples $\hat{\Theta}^W \in (-\pi, \pi]$ on $\mathcal{G}' \supset \mathcal{G}$. In DSS, motivated by extensive studies on *quality maps*, in particular, *maximum phase gradient maps* [1, Section 3.3.4], we classify all wrapped samples into reliable and unreliable classes on the basis of the wrapped phase difference. Then we smooth Θ^W by using convex optimization without changing any information about reliable wrapped samples. Finally, we construct θ_{f^*} , as an estimate of Θ , by applying SPS and APU to the denoised wrapped phase $\hat{\Theta}^W$ obtained in DSS.

This paper is organized as follows. Section II introduces bivariate spline functions on triangles. Section III-A presents the main idea of the proposed 2D phase unwrapping scheme based on SPS and APU. Section III-B and Section III-C respectively explain the details of SPS and APU. Section III-D introduces DSS and Section III-E shows the overall steps of the proposed scheme. Section IV demonstrates the effectiveness of the proposed scheme in application to InSAR terrain height estimation. Finally Section V concludes this paper.

The proposed scheme is not only based on the traditional ideas in the existing phase unwrapping techniques but also based on powerful mathematical ideas, e.g., *spline smoothing*, *convex optimization*, and *computer algebra*. For self-containedness and readability, comprehensive introductions to these ideas are also presented in Appendices.

Notation: Let \mathbb{Z} , \mathbb{Z}_+ , \mathbb{Z}_{++} , \mathbb{R} , \mathbb{R}_+ , \mathbb{R}_{++} and \mathbb{C} be the sets of all integers, non-negative integers, positive integers, real numbers, non-negative real numbers, positive real numbers, and complex numbers, respectively. We use $i \in \mathbb{C}$ to denote the imaginary unit, i.e., $i^2 = -1$, and use $i \in \mathbb{Z}_+$ and $j \in \mathbb{Z}_+$ for general indices. For any set S , $\text{card}(S)$ stands for its cardinal number. For $\rho \in \mathbb{Z}_+$, $C^\rho(\Omega)$ stands for the set of all ρ -times continuously differentiable real-valued functions over a simply connected region $\Omega \subset \mathbb{R}^2$. A boldface letter expresses a vector or a matrix. For any vector $\mathbf{x} \in \mathbb{R}^n$ and matrix $\mathbf{X} \in \mathbb{R}^{n \times m}$, $[\mathbf{x}]_i$ and $[\mathbf{X}]_{i,j}$ respectively denote the i th component of \mathbf{x} and the (i, j) entry of \mathbf{X} . For $p > 0$ and $\mathbf{w} \in \mathbb{R}_{++}^n$, the ℓ_p (quasi-)norm and the weighted ℓ_p (quasi-)norm of $\mathbf{x} \in \mathbb{R}^n$ are respectively defined as $\|\mathbf{x}\|_p := \sqrt[p]{\sum_{i=1}^n |\mathbf{x}]_i|^p}$ and $\|\mathbf{x}\|_{p, \mathbf{w}} := \sqrt[p]{\sum_{i=1}^n [\mathbf{w}]_i |\mathbf{x}]_i|^p}$ (Note: $\|\cdot\|_p$ and $\|\cdot\|_{p, \mathbf{w}}$ satisfy the condition of the norm in \mathbb{R}^n if $p \geq 1$).

II. BIVARIATE SPLINE FUNCTIONS ON TRIANGULATIONS

We restrict ourselves to partitioning a polygonal domain $\Omega \subset \mathbb{R}^2$ into triangles because these have the most flexibility with respect to the resolution of the discretization in Ω .

Define a triangle $\mathcal{T} \subset \mathbb{R}^2$, by specifying three vertices $\mathbf{v}_k := (x_k, y_k) \in \mathbb{R}^2$ ($k = 1, 2, 3$) which are not arranged linearly, i.e., $\varrho := x_1y_2 - y_1x_2 + x_2y_3 - y_2x_3 + x_3y_1 - y_3x_1 \neq 0$, as

$$\begin{aligned} \mathcal{T} &:= \langle \mathbf{v}_1, \mathbf{v}_2, \mathbf{v}_3 \rangle \\ &:= \left\{ r\mathbf{v}_1 + s\mathbf{v}_2 + t\mathbf{v}_3 \in \mathbb{R}^2 \mid \begin{array}{l} r, s, t \in [0, 1] \\ r + s + t = 1 \end{array} \right\}. \end{aligned}$$

Let $\Delta := \{\mathcal{T}_i\}_{i=1}^N$ be a collection of triangles $\mathcal{T}_i \subset \mathbb{R}^2$ whose union forms a simply connected closed region $\Omega \subset \mathbb{R}^2$, i.e., $\bigcup_{i=1}^N \mathcal{T}_i = \Omega$. If, for any pair of triangles $\mathcal{T}_i \in \Delta$ and $\mathcal{T}_j \in \Delta$ ($i \neq j$), $\mathcal{T}_i \cap \mathcal{T}_j$ is either empty or a common edge or a common vertex, the collection Δ is called a *regular triangulation*. Given a regular triangulation Δ and $\rho, d \in \mathbb{Z}_+$ s.t. $0 \leq \rho < d$, define

$$S_d^\rho(\Delta) := \{f \in C^\rho(\Omega) \mid \forall \mathcal{T}_i \in \Delta \quad f = f_i \in \mathbb{P}_d \text{ over } \mathcal{T}_i\}$$

as the set of all bivariate spline functions of degree d and smoothness ρ on Δ , where \mathbb{P}_d stands for the set of all bivariate polynomials whose degree is d at most, i.e., $\mathbb{P}_d := \{f : \mathbb{R}^2 \rightarrow \mathbb{R} : (x, y) \mapsto \sum_{i=0}^d \sum_{j=0}^{d-i} c_{i,j} x^i y^j \mid c_{i,j} \in \mathbb{R}\}$.

For $\mathcal{T} = \langle \mathbf{v}_1, \mathbf{v}_2, \mathbf{v}_3 \rangle$ s.t. $\mathbf{v}_k = (x_k, y_k) \in \mathbb{R}^2$ ($k = 1, 2, 3$), every $(x, y) \in \mathbb{R}^2$ can be expressed uniquely in the form

$$(x, y) = r\mathbf{v}_1 + s\mathbf{v}_2 + t\mathbf{v}_3 \quad \text{s.t. } r + s + t = 1,$$

where (r, s, t) is called *barycentric coordinate* of (x, y) with respect to \mathcal{T} [46], [47] and expressed as

$$\left. \begin{aligned} r &= ((y_2 - y_3)x - (x_2 - x_3)y + x_2y_3 - y_2x_3)/\varrho \\ s &= ((y_3 - y_1)x - (x_3 - x_1)y + x_3y_1 - y_3x_1)/\varrho \\ t &= ((y_1 - y_2)x - (x_1 - x_2)y + x_1y_2 - y_1x_2)/\varrho \end{aligned} \right\}.$$

By using the above expression of (x, y) , the *Bernstein-Bézier polynomial* of degree d is defined, for \mathcal{T} and $(l, m, n) \in \mathbb{Z}_+^3$ satisfying $l + m + n = d$, as

$$B_{l,m,n}^{\mathcal{T}} : \mathbb{R}^2 \rightarrow \mathbb{R} : (x, y) \mapsto \frac{d!}{l!m!n!} r^l s^m t^n.$$

It is known that $\{B_{l,m,n}^{\mathcal{T}} \mid (l, m, n) \in \mathbb{Z}_+^3 \text{ and } l + m + n = d\}$ is a basis of \mathbb{P}_d , and hence any piecewise polynomial f , whose restriction f_i to $\mathcal{T}_i \in \Delta$ satisfies $f_i \in \mathbb{P}_d$ ($i = 1, 2, \dots, N$), can be expressed uniquely as

$$f_i(x, y) = f_{\mathcal{T}_i}(r, s, t) := \sum_{l+m+n=d} c_{l,m,n}^{\mathcal{T}_i} \frac{d!}{l!m!n!} r^l s^m t^n, \quad (7)$$

where (r, s, t) is barycentric coordinate with respect to \mathcal{T}_i . Such a representation of piecewise polynomials is called the *Bernstein-Bézier form* (or *B-form* for short), and $c_{l,m,n}^{\mathcal{T}_i} \in \mathbb{R}$ is called the *Bernstein-Bézier coefficient* (or *B-coefficient*). By using the B-coefficient vector $\mathbf{c} := \text{vec}(c_{l,m,n}^{\mathcal{T}_i})_{l+m+n=d}^{i=1,2,\dots,N}$ of such f , Lai [48] gave a matrix \mathbf{H} for characterization $f \in S_d^\rho(\Delta) \Leftrightarrow \mathbf{H}\mathbf{c} = \mathbf{0}$. Such a matrix \mathbf{H} is deduced as follows.

Fact 1 ([48]): Let $\mathcal{T}_1 := \langle \mathbf{v}_1, \mathbf{v}_2, \mathbf{v}_3 \rangle$, $\mathcal{T}_2 := \langle \mathbf{v}_1, \mathbf{v}_2, \mathbf{v}_4 \rangle$ and let (r_4, s_4, t_4) be barycentric coordinate of \mathbf{v}_4 with respect

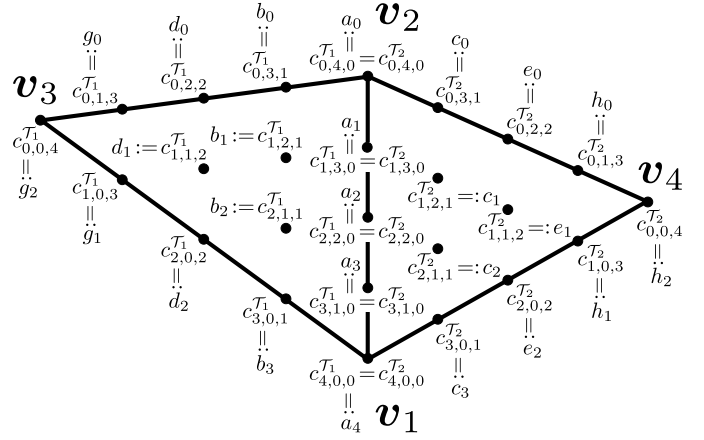


Fig. 1. Example of the Bézier net of a bivariate spline function f of degree $d = 4$ on a regular triangulation $\Delta = \{\mathcal{T}_1, \mathcal{T}_2\}$, where $\mathcal{T}_1 = \langle \mathbf{v}_1, \mathbf{v}_2, \mathbf{v}_3 \rangle$ and $\mathcal{T}_2 = \langle \mathbf{v}_1, \mathbf{v}_2, \mathbf{v}_4 \rangle$.

to \mathcal{T}_1 . Suppose that $f : \mathcal{T}_1 \cup \mathcal{T}_2 \rightarrow \mathbb{R}$ can be expressed as (7) over \mathcal{T}_i ($i = 1, 2$). Then $f \in S_d^\rho(\{\mathcal{T}_1, \mathcal{T}_2\})$ if and only if

$$L_1^{\lceil \frac{\rho}{2} \rceil}(c_{l,m,n}^{\mathcal{T}_1}) = L_2^{\lfloor \frac{\rho}{2} \rfloor}(c_{l,m,n}^{\mathcal{T}_2})$$

for all $n = 0, 1, \dots, \rho$ and $l + m = d - n$, where $\lceil \cdot \rceil$ and $\lfloor \cdot \rfloor$ are respectively the ceiling and floor functions, i.e.,

$$\left. \begin{aligned} \lceil x \rceil &:= \min \{z \in \mathbb{Z} \mid z \geq x\} \\ \lfloor x \rfloor &:= \max \{z \in \mathbb{Z} \mid z \leq x\} \end{aligned} \right\},$$

and $L_i^k(c_{l,m,n}^{\mathcal{T}_i}) \in \mathbb{R}$ ($l + m + n = d$, $i = 1, 2$ and $k \in \mathbb{Z}_+$) are defined recursively by $L_i^0(c_{l,m,n}^{\mathcal{T}_i}) := c_{l,m,n}^{\mathcal{T}_i}$ and

$$\begin{aligned} L_i^k(c_{l,m,n}^{\mathcal{T}_i}) &:= \frac{r_4}{(-t_4)^{i-1}} L_i^{k-1}(c_{l+1,m,n-1}^{\mathcal{T}_i}) \\ &\quad + \frac{s_4}{(-t_4)^{i-1}} L_i^{k-1}(c_{l,m+1,n-1}^{\mathcal{T}_i}) + \frac{t_4}{(t_4)^{2i-2}} L_i^{k-1}(c_{l,m,n}^{\mathcal{T}_i}) \end{aligned}$$

for $k \geq 1$. \square

Actually, we can use a more compact expression by removing some redundant components in \mathbf{c} as follows.

Remark 1 (A Compact Expression of the B-Coefficients): Let us consider a simple example where a regular triangulation Δ has only two triangles $\mathcal{T}_1 := \langle \mathbf{v}_1, \mathbf{v}_2, \mathbf{v}_3 \rangle$ and $\mathcal{T}_2 := \langle \mathbf{v}_1, \mathbf{v}_2, \mathbf{v}_4 \rangle$, i.e., $\Delta := \{\mathcal{T}_1, \mathcal{T}_2\}$ and $\mathcal{T}_1 \cup \mathcal{T}_2 =: \Omega$. Suppose that f is a bivariate spline function of degree $d = 4$ on Δ . Then, since there exist fifteen combinations for $(l, m, n) \in \mathbb{Z}_+^3$ s.t. $l + m + n = 4$, the size of the B-coefficient vector is 30, i.e., $\mathbf{c} := \text{vec}(c_{l,m,n}^{\mathcal{T}_i})_{l+m+n=4}^{i=1,2} \in \mathbb{R}^{30}$. Meanwhile, in spline function theory [46], [47], [49]–[52], the B-coefficients $c_{l,m,n}^{\mathcal{T}_1}$ and $c_{l,m,n}^{\mathcal{T}_2}$ are respectively assigned to $\frac{l}{l+m+n}\mathbf{v}_1 + \frac{m}{l+m+n}\mathbf{v}_2 + \frac{n}{l+m+n}\mathbf{v}_3 \in \mathcal{T}_1$ and $\frac{l}{l+m+n}\mathbf{v}_1 + \frac{m}{l+m+n}\mathbf{v}_2 + \frac{n}{l+m+n}\mathbf{v}_4 \in \mathcal{T}_2$ (such a representation is called the *Bézier net* [49]) as shown in Fig. 1 where we see that $c_{i,4-i,0}^{\mathcal{T}_1}$ and $c_{i,4-i,0}^{\mathcal{T}_2}$ ($i = 0, 1, 2, 3, 4$) are assigned to the same location. This corresponds to the characterization of $f \in S_d^0(\Delta)$ in Fact 1 by

$$c_{i,4-i,0}^{\mathcal{T}_1} = c_{i,4-i,0}^{\mathcal{T}_2} \quad (i = 0, 1, 2, 3, 4).$$

Hence by imposing $a_i := c_{i,4-i,0}^{\mathcal{T}_1} = c_{i,4-i,0}^{\mathcal{T}_2}$ ($i = 0, 1, 2, 3, 4$) on the B-coefficients for \mathcal{T}_1 and \mathcal{T}_2 , we can guarantee $f \in$

$\mathcal{S}_4^0(\Delta)$ and can reduce the size of the B-coefficient vector from 30 to 25, i.e., with the use of $a_i, b_i, c_i, d_i, e_i, g_i,$ and h_i in Fig. 1, we can redefine the B-coefficient vector as $\mathbf{c} := \text{vec}((a_i)_{i=0}^4, (b_i, c_i)_{i=0}^3, (d_i, e_i, g_i, h_i)_{i=0}^2) \in \mathbb{R}^{25}$. Then $f \in \mathcal{S}_4^0(\Delta)$ on each triangle \mathcal{T}_i can be expressed, in terms of barycentric coordinate (r, s, t) with respect to \mathcal{T}_i , as (8) and (9). In particular, the values of f at vertices \mathbf{v}_i ($i = 1, 2, 3, 4$) are easily determined by

$$\left. \begin{aligned} f(\mathbf{v}_1) &= f_{\mathcal{T}_1}(1, 0, 0) = f_{\mathcal{T}_2}(1, 0, 0) = a_4 \\ f(\mathbf{v}_2) &= f_{\mathcal{T}_1}(0, 1, 0) = f_{\mathcal{T}_2}(0, 1, 0) = a_0 \\ f(\mathbf{v}_3) &= f_{\mathcal{T}_1}(0, 0, 1) = g_2 \\ f(\mathbf{v}_4) &= f_{\mathcal{T}_2}(0, 0, 1) = h_2 \end{aligned} \right\}. \quad (10)$$

From Fact 1, f satisfies $f \in \mathcal{S}_4^1(\Delta)$ if and only if

$$r_4 a_{i+1} + s_4 a_i + t_4 b_i = c_i \quad (i = 0, 1, 2, 3), \quad (11)$$

where (r_4, s_4, t_4) is barycentric coordinate of \mathbf{v}_4 with respect to \mathcal{T}_1 , i.e., $r_4 \mathbf{v}_1 + s_4 \mathbf{v}_2 + t_4 \mathbf{v}_3 = \mathbf{v}_4$ and $r_4 + s_4 + t_4 = 1$. Similarly f satisfies $f \in \mathcal{S}_4^2(\Delta)$ if and only if (11) and

$$t_4(r_4 b_{i+1} + s_4 b_i + t_4 d_i) = -r_4 c_{i+1} - s_4 c_i + e_i \quad (i = 0, 1, 2). \quad (12)$$

Finally, from (11) and (12), we can construct a matrix \mathbf{H} , for each $\rho = 1, 2$, satisfying $f \in \mathcal{S}_4^\rho(\Delta) \Leftrightarrow \mathbf{H}\mathbf{c} = \mathbf{0}$. \square

III. ALGEBRAIC RECOVERY OF 2D UNWRAPPED PHASE

A. General Idea of the Proposed Scheme

In this section, we propose an algebraic approach for high-resolution 2D phase unwrapping. We estimate the unwrapped phase Θ as a continuous function defined over Ω unlike many existing algorithms (see Appendix A). In our previous works [41], [42], by using *Poincaré's lemma* [53], we clarified the condition for the unique existence of the continuous phase function $\theta_f \in C^2(\Omega)$ of a complex function $f := f_{(0)} + \iota f_{(1)} : \Omega \rightarrow \mathbb{C}$ s.t. $f_{(k)} \in C^2(\Omega)$ ($k = 0, 1$).

Fact 2 ([41]): Let Ω be a simply connected closed region on \mathbb{R}^2 . Suppose that $f_{(k)} : \Omega \rightarrow \mathbb{R}$ ($k = 0, 1$) are twice continuously differentiable functions, i.e., $f_{(k)} \in C^2(\Omega)$, and satisfy $f(x, y) := f_{(0)}(x, y) + \iota f_{(1)}(x, y) \neq 0$ for all $(x, y) \in \Omega$. Then for arbitrarily fixed $(x_0, y_0) \in \Omega$ and θ_0 satisfying $f(x_0, y_0) = |f(x_0, y_0)|e^{i\theta_0}$, the following hold.

- (i) There exists a unique continuous function $\theta_f \in C^2(\Omega)$ satisfying $\theta_f(x_0, y_0) = \theta_0$ and

$$\left. \begin{aligned} \frac{\partial \theta_f}{\partial x}(x, y) &= \Im \left[\frac{\frac{\partial f_{(0)}}{\partial x}(x, y) + \iota \frac{\partial f_{(1)}}{\partial x}(x, y)}{f_{(0)}(x, y) + \iota f_{(1)}(x, y)} \right] \\ \frac{\partial \theta_f}{\partial y}(x, y) &= \Im \left[\frac{\frac{\partial f_{(0)}}{\partial y}(x, y) + \iota \frac{\partial f_{(1)}}{\partial y}(x, y)}{f_{(0)}(x, y) + \iota f_{(1)}(x, y)} \right] \end{aligned} \right\} \quad (13)$$

for all $(x, y) \in \Omega$, where $\Im(c)$ stands for the imaginary part of $c \in \mathbb{C}$. θ_f satisfies

$$f(x, y) = |f(x, y)|e^{i\theta_f(x, y)} \quad \text{for all } (x, y) \in \Omega.$$

- (ii) Let $\Upsilon : [a, b] \rightarrow \Omega$ be a piecewise C^1 path s.t. $\Upsilon(a) = (x_0, y_0)$ and $\Upsilon(b) = (x_1, y_1) \in \Omega$. Then we have

$$\theta_f(x_1, y_1) = \theta_0 + \int_a^b \Im \left[\frac{F'_{(0)}(\tau) + \iota F'_{(1)}(\tau)}{F_{(0)}(\tau) + \iota F_{(1)}(\tau)} \right] d\tau,$$

where $F_{(k)}(\tau) := f_{(k)}(\Upsilon(\tau))$ ($k = 0, 1$). \square

Remark 2 (Note on Equation (13)): Note that

$$\Im \left[\frac{\frac{\partial f_{(0)}}{\partial x}(x, y) + \iota \frac{\partial f_{(1)}}{\partial x}(x, y)}{f_{(0)}(x, y) + \iota f_{(1)}(x, y)} \right] = \frac{\partial}{\partial x} \left[\arctan \left(\frac{f_{(1)}(x, y)}{f_{(0)}(x, y)} \right) \right]$$

$$\Im \left[\frac{\frac{\partial f_{(0)}}{\partial y}(x, y) + \iota \frac{\partial f_{(1)}}{\partial y}(x, y)}{f_{(0)}(x, y) + \iota f_{(1)}(x, y)} \right] = \frac{\partial}{\partial y} \left[\arctan \left(\frac{f_{(1)}(x, y)}{f_{(0)}(x, y)} \right) \right]$$

holds at every $(x, y) \in \Omega$ satisfying $f_{(0)}(x, y) \neq 0$, where $\arctan : \mathbb{R} \rightarrow (-\pi/2, \pi/2)$ returns the principal value of the inverse tangent, i.e., $\tan(\arctan(x)) = x$ for all $x \in \mathbb{R}$. \square

Trying to estimate Θ by $\theta_f \in C^2(\Omega)$, from Fact 2, we can reduce the estimation problem of Θ to those of $f_{(0)} \in C^2(\Omega)$ and $f_{(1)} \in C^2(\Omega)$ which respectively approximate $\cos \Theta$ and $\sin \Theta$. In particular, under the assumption that phase noise ν is not significant in (1), $f_{(0)}$ and $f_{(1)}$ are desired to interpolate $\cos(\Theta^W(x, y)) \approx \cos(\Theta(x, y))$ and $\sin(\Theta^W(x, y)) \approx \sin(\Theta(x, y))$, respectively, at every sampling point $(x, y) \in \mathcal{G}$. Moreover, on the basis of the idea of *functional data analysis* [35]–[37], we search for $f_{(0)}$ and $f_{(1)}$ which are smooth. Here the word “smooth” means that the energy of local change, i.e., the L_2 norm of the second order partial derivative, is small over Ω . Therefore we design a smooth continuous phase function θ_f by minimizing the energy of local change of $f_{(k)}$ ($k = 0, 1$):

$$\iint_{\Omega} \left[\left| \frac{\partial^2 f_{(k)}}{\partial x^2} \right|^2 + 2 \left| \frac{\partial^2 f_{(k)}}{\partial x \partial y} \right|^2 + \left| \frac{\partial^2 f_{(k)}}{\partial y^2} \right|^2 \right] dx dy \quad (14)$$

in a suitable functional space subject to $|f(x, y)| > 0$ for all $(x, y) \in \Omega$ and²

$$\left. \begin{aligned} f_{(0)}(x, y) &= \cos(\Theta^W(x, y)) \\ f_{(1)}(x, y) &= \sin(\Theta^W(x, y)) \end{aligned} \right\} \quad \text{for all } (x, y) \in \mathcal{G}. \quad (15)$$

We can guarantee that θ_f satisfies $W(\theta_f(x, y)) = \Theta^W(x, y)$ for all $(x, y) \in \mathcal{G}$ if (15) and $|f(x, y)| > 0$ for all $(x, y) \in \Omega$.

²Of course, condition (15) can be generalized in a natural way if amplitude information at every sampling point $(x, y) \in \mathcal{G}$ is available.

$$f_1(x, y) = f_{\mathcal{T}_1}(r, s, t) = a_4 r^4 + 4a_3 r^3 s + 4b_3 r^3 t + 6a_2 r^2 s^2 + 12b_2 r^2 s t + 6d_2 r^2 t^2 + 4a_1 r s^3 + 12b_1 r s^2 t + 12d_1 r s t^2 + 4g_1 r t^3 + a_0 s^4 + 4b_0 s^3 t + 6d_0 s^2 t^2 + 4g_0 s t^3 + g_2 t^4 \quad (8)$$

$$f_2(x, y) = f_{\mathcal{T}_2}(r, s, t) = a_4 r^4 + 4a_3 r^3 s + 4c_3 r^3 t + 6a_2 r^2 s^2 + 12c_2 r^2 s t + 6e_2 r^2 t^2 + 4a_1 r s^3 + 12c_1 r s^2 t + 12e_1 r s t^2 + 4h_1 r t^3 + a_0 s^4 + 4c_0 s^3 t + 6e_0 s^2 t^2 + 4h_0 s t^3 + h_2 t^4 \quad (9)$$

Motivated by Fact 2 and the successful utilization of spline functions in functional data analysis [47], [49]–[52], [54]–[58], (see, e.g., Appendix B on a certain optimality of spline functions), we adopt the bivariate spline space $\mathcal{S}_d^2(\Delta)$ ($d \geq 3$) as the set of all possible candidates of $f_{(k)}$.

As a result, we propose the following 2D phase unwrapping scheme whose core consists of *SPLine Smoothing (SPS)* and *Algebraic Phase Unwrapping (APU)*.

SPS: Find $f_{(k)}^* \in \mathcal{S}_d^2(\Delta) \subset C^2(\Omega)$ ($k = 0, 1$ and $d \geq 3$) which minimize (14) subject to (15).

APU: For any point of interest $(x, y) \in \Omega$, compute the value of $\theta_{f^*}(x, y)$ defined in Fact 2(ii) along a suitable piecewise C^1 path Υ .

Note that SPS is a convex relaxation of an original optimization problem, defined with (14) and (15), which requires an additional condition $f_{(0)}(x, y) + \nu f_{(1)}(x, y) \neq 0$ for all $(x, y) \in \Omega$. Fortunately, if the observed wrapped phase Θ^W is not contaminated by severe phase noise and sufficiently many sampling points are available to capture the geometric feature of Θ , the solution $(f_{(0)}^*, f_{(1)}^*)$ of this relaxed problem tends to automatically satisfy the additional condition. If there exists $(x, y) \in \Omega$ s.t. $f_{(0)}^*(x, y) + \nu f_{(1)}^*(x, y) = 0$, we use a denoising step proposed in Section III-D to avoid the occurrence of zeros.

B. SPLine Smoothing (SPS)

Let $\mathbf{c}_{(k)}$ ($k = 0, 1$) be the B-coefficient vectors of $f_{(k)} \in \mathcal{S}_d^0(\Delta)$ (see Remark 1). Then the energy of local change in (14) can be expressed as $\mathbf{c}_{(k)}^T \mathbf{Q} \mathbf{c}_{(k)}$ [59, Theorem 1] (see Appendix C), where \mathbf{Q} is a symmetric positive semidefinite matrix. The condition $f_{(k)} \in \mathcal{S}_d^2(\Delta) (\subset \mathcal{S}_d^0(\Delta))$ is equivalent to $\mathbf{H} \mathbf{c}_{(k)} = \mathbf{0}$ as shown in Remark 1 and condition (15) can be expressed as $\mathcal{I} \mathbf{c}_{(k)} = \mathbf{d}_{(k)}$ in terms of

$$\left. \begin{aligned} \mathbf{d}_{(0)} &:= \text{vec}(\cos(\Theta^W(x, y)))_{(x, y) \in \mathcal{G}} \\ \mathbf{d}_{(1)} &:= \text{vec}(\sin(\Theta^W(x, y)))_{(x, y) \in \mathcal{G}} \end{aligned} \right\}$$

and a sparse matrix \mathcal{I} . Indeed, if we assume that

$$\text{every } (x, y) \in \mathcal{G} \text{ is a vertex of some } \mathcal{T} \in \Delta, \quad (16)$$

each row vector of \mathcal{I} has only one non-zero component ‘1’ (see, e.g., (10)). As a result, SPS in the proposed scheme is reduced to the following convex optimization problem, say SPS again, for the B-coefficient vector $\mathbf{c}_{(k)}$:

SPS: Find $\mathbf{c}_{(k)}^*$ ($k = 0, 1$) minimizing

$$\mathbf{c}_{(k)}^T \mathbf{Q} \mathbf{c}_{(k)}$$

subject to $\mathbf{H} \mathbf{c}_{(k)} = \mathbf{0}$ and $\mathcal{I} \mathbf{c}_{(k)} = \mathbf{d}_{(k)}$.

Moreover, by considering the reliability of wrapped samples influenced by phase noise ν , we can relax SPS as a generalized Hermite-Birkhoff interpolation problem [57]:

SPS+: Find $\mathbf{c}_{(k)}^*$ ($k = 0, 1$) minimizing

$$\mathbf{c}_{(k)}^T \mathbf{Q} \mathbf{c}_{(k)}$$

subject to $\mathbf{H} \mathbf{c}_{(k)} = \mathbf{0}$ and $-\epsilon_{(k)} \leq \mathcal{I} \mathbf{c}_{(k)} - \mathbf{d}_{(k)} \leq \epsilon_{(k)}$,

where $\epsilon_{(k)} := \text{vec}(\epsilon_{(k)}(x, y))_{(x, y) \in \mathcal{G}} \in \mathbb{R}_+^{\text{card}(\mathcal{G})}$ ($k = 0, 1$) are the acceptable interpolation errors designed to be small

if the wrapped phase $\Theta^W(x, y)$ is reliable at $(x, y) \in \mathcal{G}$, and relatively large otherwise. SPS and SPS+ can be solved by quadratic programming solvers, e.g., in [60]–[62] if the constraints are feasible.

Even if the constraint in SPS (or SPS+) is infeasible, it can be relaxed in the following sense of hierarchical convex optimization problem:

SPS++: Find $\mathbf{c}_{(k)}^*$ ($k = 0, 1$) minimizing

$$\begin{aligned} &\mathbf{c}_{(k)}^{*T} \mathbf{Q} \mathbf{c}_{(k)}^* \\ &\text{subject to } \mathbf{c}_{(k)}^* \in \underset{\mathbf{H} \mathbf{c}_{(k)} = \mathbf{0}}{\text{argmin}} \|\mathcal{I} \mathbf{c}_{(k)} - \mathbf{d}_{(k)}\|_2^2. \end{aligned}$$

SPS++ can be solved by *hybrid steepest descent method* [63]–[68].

C. Algebraic Phase Unwrapping (APU)

Let $\Delta := \{\mathcal{T}_i := \langle \mathbf{v}_1^{(i)}, \mathbf{v}_2^{(i)}, \mathbf{v}_3^{(i)} \rangle\}_{i=1}^N$ be a regular triangulation satisfying (16), and let $\theta_0 \in \mathbb{R}$ satisfy $f^*(\mathbf{v}_1^{(1)}) := f_{(0)}^*(\mathbf{v}_1^{(1)}) + \nu f_{(1)}^*(\mathbf{v}_1^{(1)}) = |f^*(\mathbf{v}_1^{(1)})| e^{i\theta_0}$. Suppose that we are interested in the continuous phase function θ_{f^*} of f^* at $\mathbf{v}_2^{(K)}$ ($1 \leq K \leq N$), where we assume, without loss of generality, $\mathbf{v}_1^{(i+1)} = \mathbf{v}_2^{(i)}$ ($i = 1, 2, \dots, K-1$) by renumbering the indices of triangles and their vertices if necessary. Define a piecewise C^1 path $\Upsilon: [0, K] \rightarrow \bigcup_{i=1}^K \mathcal{T}_i$ by

$$\Upsilon(\tau) := (\tau - i + 1)(\mathbf{v}_2^{(i)} - \mathbf{v}_1^{(i)}) + \mathbf{v}_1^{(i)} \quad \text{for } \tau \in [i-1, i],$$

and then, from Fact 2(ii), $\theta_{f^*}(\mathbf{v}_2^{(K)})$ is expressed as

$$\theta_{f^*}(\mathbf{v}_2^{(K)}) = \theta_0 + \int_0^K \Im \left[\frac{F'_{(0)}(\tau) + \nu F'_{(1)}(\tau)}{F_{(0)}(\tau) + \nu F_{(1)}(\tau)} \right] d\tau, \quad (17)$$

where $F_{(k)}(\tau) := f_{(k)}^*(\Upsilon(\tau))$ ($k = 0, 1$). In this case, the integral in (17) is expressed as

$$\begin{aligned} &\sum_{i=1}^K \int_{i-1}^i \Im \left[\frac{F'_{(0)}(\tau) + \nu F'_{(1)}(\tau)}{F_{(0)}(\tau) + \nu F_{(1)}(\tau)} \right] d\tau \\ &= \sum_{i=1}^K \int_0^1 \Im \left[\frac{F_{(0)}^{(i)'}(\tau) + \nu F_{(1)}^{(i)'}(\tau)}{F_{(0)}^{(i)}(\tau) + \nu F_{(1)}^{(i)}(\tau)} \right] d\tau, \end{aligned} \quad (18)$$

where $F_{(k)}^{(i)}(\tau) := F_{(k)}(\tau + i - 1) = f_{(k)}^*(\Upsilon(\tau + i - 1)) = f_{(k), \mathcal{T}_i}^*(1 - \tau, \tau, 0)$ ($\tau \in [0, 1]$, $k = 0, 1$ and $i = 1, 2, \dots, K$) are univariate polynomials of degree d at most. For example, if $f_{(k)}^* \in \mathcal{S}_4^2(\Delta)$, by using its B-coefficients $(c_{l,m,n}^{\mathcal{T}_i, (k)})_{l+m+n=4}$, $F_{(k)}^{(i)}$ ($k = 0, 1$ and $i = 1, 2, \dots, K$) are expressed as

$$\begin{aligned} F_{(k)}^{(i)}(\tau) &= f_{(k), \mathcal{T}_i}^*(1 - \tau, \tau, 0) \\ &= c_{4,0,0}^{\mathcal{T}_i, (k)} (1 - \tau)^4 + 4c_{3,1,0}^{\mathcal{T}_i, (k)} \tau(1 - \tau)^3 \\ &\quad + 6c_{2,2,0}^{\mathcal{T}_i, (k)} \tau^2(1 - \tau)^2 + 4c_{1,3,0}^{\mathcal{T}_i, (k)} \tau^3(1 - \tau) + c_{0,4,0}^{\mathcal{T}_i, (k)} \tau^4 \\ &= \left(c_{4,0,0}^{\mathcal{T}_i, (k)} - 4c_{3,1,0}^{\mathcal{T}_i, (k)} + 6c_{2,2,0}^{\mathcal{T}_i, (k)} - 4c_{1,3,0}^{\mathcal{T}_i, (k)} + c_{0,4,0}^{\mathcal{T}_i, (k)} \right) \tau^4 \\ &\quad - 4 \left(c_{4,0,0}^{\mathcal{T}_i, (k)} - 3c_{3,1,0}^{\mathcal{T}_i, (k)} + 3c_{2,2,0}^{\mathcal{T}_i, (k)} - c_{1,3,0}^{\mathcal{T}_i, (k)} \right) \tau^3 \\ &\quad + 6 \left(c_{4,0,0}^{\mathcal{T}_i, (k)} - 2c_{3,1,0}^{\mathcal{T}_i, (k)} + c_{2,2,0}^{\mathcal{T}_i, (k)} \right) \tau^2 \\ &\quad - 4 \left(c_{4,0,0}^{\mathcal{T}_i, (k)} - c_{3,1,0}^{\mathcal{T}_i, (k)} \right) \tau + c_{4,0,0}^{\mathcal{T}_i, (k)}. \end{aligned}$$

Input: $P_{(0)}(\tau) \in \mathbb{R}[\tau]$, $P_{(1)}(\tau) \in \mathbb{R}[\tau]$ and $a \in \mathbb{R}$

Output: $(\Psi_j(\tau))_{j=0}^q$

- 1: $\Psi_0(\tau) \leftarrow \frac{P_{(0)}(\tau)}{(\tau-a)^{e_0}}$ (e_0 is the order of a as a zero of polynomial $P_{(0)}$)
- 2: $\Psi_1(\tau) \leftarrow \frac{P_{(1)}(\tau)}{(\tau-a)^{e_1}}$ (e_1 is the order of a as a zero of polynomial $P_{(1)}$)
- 3: $j \leftarrow 1$
- 4: **while** $\deg(\Psi_j) \geq 1$ ($\deg(\Psi_j)$ is the degree of polynomial Ψ_j) **do**
- 5: $\Psi_{j+1} \leftarrow -\text{rem}(\Psi_{j-1}, \Psi_j)$
($\text{rem}(\Psi_{j-1}, \Psi_j)$ is the remainder of division of Ψ_{j-1} by Ψ_j)
- 6: $j \leftarrow j + 1$
- 7: **end while**
- 8: $q \leftarrow j$
- 9: Return $(\Psi_j(\tau))_{j=0}^q$

Fig. 2. Algorithm generating the polynomials $(\Psi_j(\tau))_{j=0}^q$ in Fact 3 for APU.

Since $F_{(k)}^{(i)}(\tau) \in \mathbb{R}[\tau]$ ($k = 0, 1$) are univariate polynomials, all integrals in (18) can be computed analytically by the following method called *algebraic phase unwrapping* [38]–[42].

Fact 3 ([41]): Let $P_{(k)}(\tau) \in \mathbb{R}[\tau]$ ($k = 0, 1$) be nonzero univariate real polynomials, and let $P(\tau) := P_{(0)}(\tau) + \iota P_{(1)}(\tau) \in \mathbb{C}[\tau]$ be a univariate complex polynomial satisfying $P(\tau) \neq 0$ for all $\tau \in [a, b]$. Then, for every $\tau^* \in (a, b]$, we have

$$\int_a^{\tau^*} \Im \left[\frac{P'_{(0)}(\tau) + \iota P'_{(1)}(\tau)}{P_{(0)}(\tau) + \iota P_{(1)}(\tau)} \right] d\tau = \begin{cases} \arctan(\mathcal{Q}(\tau^*)) + [V(\Psi(\tau^*)) - V(\Psi(a))] \pi & \text{if } P_{(0)}(\tau^*) \neq 0; \\ \frac{\pi}{2} + [V(\Psi(\tau^*)) - V(\Psi(a))] \pi & \text{if } P_{(0)}(\tau^*) = 0; \\ - \begin{cases} \arctan(\mathcal{Q}(a)) & \text{if } P_{(0)}(a) \neq 0; \\ \text{sgn}(\Psi_0(a)\Psi_1(a)) \frac{\pi}{2} & \text{if } P_{(0)}(a) = 0, \end{cases} \end{cases} \quad (19)$$

where $\mathcal{Q}(\tau) := P_{(1)}(\tau)/P_{(0)}(\tau)$, $\text{sgn}(x) := x/|x|$ for $x \neq 0$, $\text{sgn}(x) := 0$ for $x = 0$, and $V(\Psi(\tau^*)), V(\Psi(a)) \in \mathbb{Z}_+$ are the numbers of sign changes, at $\tau = \tau^*$ and $\tau = a$, in the polynomial sequence $(\Psi_j(\tau))_{j=0}^q$ generated by the algorithm in Fig. 2. If there exists some Ψ_j whose value at τ^* is $\Psi_j(\tau^*) = 0$, its sign is not counted (e.g., if $q = 5$, $\tau^* = 1$ and $(\Psi_0(1), \Psi_1(1), \Psi_2(1), \Psi_3(1), \Psi_4(1), \Psi_5(1)) = (3, -2, 5, 1, 0, -2)$, then $V(\Psi(\tau^*)) = 3$ because there are three sign changes ($3 \rightarrow -2$), ($-2 \rightarrow 5$) and ($1 \rightarrow -2$)). \square

In [41], we also proposed an alternative way, based on *subresultant* theory [69], of computation for $V(\Psi(\tau^*))$ and $V(\Psi(a))$ in (19), to resolve certain instabilities caused by polynomial division in the algorithm in Fig. 2. In this paper, we use [41, Theorem 3] for fast and stable evaluations of $V(\Psi(\tau^*))$ and $V(\Psi(a))$ in (19). For completeness, we summarize this idea in Appendix D.

Note that, under the condition $f^*(x, y) \neq 0$ for all $(x, y) \in \Omega$, we can compute $\theta_{f^*}(x, y)$ not only at $(x, y) \in \mathcal{G}$ but also at any $(x, y) \in \Omega$ by repeatedly applying algebraic phase unwrapping. Therefore, unlike many existing algorithms, the proposed 2D phase unwrapping scheme gives a smooth θ_{f^*} , as a high-resolution estimate of Θ , which is consistent with the wrapped phase, i.e., $W(\theta_{f^*}(x, y)) \approx \Theta^W(x, y)$ at $(x, y) \in \mathcal{G}$. This approach is particularly effective in the case where phase noise is relatively small as shown in the following example.

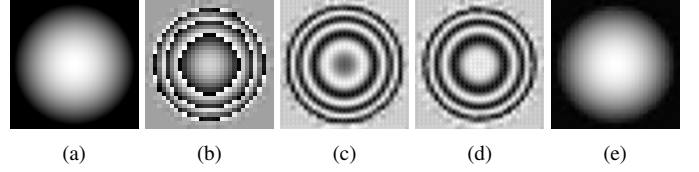


Fig. 3. Numerical example of the proposed 2D phase unwrapping (SPS and APU) (I): (a) unwrapped phase Θ (to be estimated), (b) wrapped phase Θ^W with small noise, (c) $f_{(0)}^*$ by SPS, (d) $f_{(1)}^*$ by SPS, and (e) θ_{f^*} by APU.

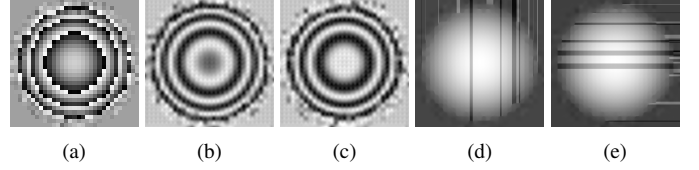


Fig. 4. Numerical example of the proposed 2D phase unwrapping (SPS and APU) (II): (a) wrapped phase Θ^W with more severe noise, (b) $f_{(0)}^*$ by SPS, (c) $f_{(1)}^*$ by SPS, (d) θ_{f^*} by APU along Υ_1 , and (e) θ_{f^*} by APU along Υ_2 .

Example 1 (2D Phase Unwrapping by SPS and APU): Suppose that the unwrapped phase

$$\Theta(x, y) := \max \left\{ 0, 20 - \frac{(x-15)^2 + (y-15)^2}{10} \right\} + \frac{\pi}{4}$$

is defined over $\Omega := [0, 30] \times [0, 30]$ as shown in Fig. 3(a). Figure 3(b) shows the observed wrapped phase $\Theta^W(x_i, y_j)$ ($\mathcal{G} := \{(x_i, y_j) := (i, j)\}_{i,j=0,1,\dots,30}$) which is contaminated by small white Gaussian noise ($\sigma^2 = 1/25$) over $\mathcal{R} := \{(x, y) \in \mathcal{G} \mid 12^2 \leq (x-15)^2 + (y-15)^2 \leq 16^2\}$ (see Section III-D-1 for the reason of this simple phase noise model). The smoothest spline functions $f_{(0)}^* \in \mathcal{S}_4^2(\Delta_{\dagger})$ and $f_{(1)}^* \in \mathcal{S}_4^2(\Delta_{\dagger})$ computed by SPS are respectively shown in Figs. 3(c) and 3(d), where $\Delta_{\dagger} := \{\mathcal{T}_{i,j}^{(1)}, \mathcal{T}_{i,j}^{(2)}, \mathcal{T}_{i,j}^{(3)}, \mathcal{T}_{i,j}^{(4)}\}_{i,j=0,1,\dots,29}$ is a *crisscross partition* constructed by cutting every rectangle $[x_i, x_{i+1}] \times [y_j, y_{j+1}] (\subset \Omega)$ into four triangles $\mathcal{T}_{i,j}^{(1)} := \langle \mathbf{v}_{i,j}, \mathbf{v}_{i,j+1}, \mathbf{v}'_{i,j} \rangle$, $\mathcal{T}_{i,j}^{(2)} := \langle \mathbf{v}_{i,j}, \mathbf{v}_{i+1,j}, \mathbf{v}'_{i,j} \rangle$, $\mathcal{T}_{i,j}^{(3)} := \langle \mathbf{v}_{i,j+1}, \mathbf{v}_{i+1,j+1}, \mathbf{v}'_{i,j} \rangle$, and $\mathcal{T}_{i,j}^{(4)} := \langle \mathbf{v}_{i+1,j}, \mathbf{v}_{i+1,j+1}, \mathbf{v}'_{i,j} \rangle$ s.t. $\mathbf{v}_{i,j} := (x_i, y_j)$ and $\mathbf{v}'_{i,j} := (\frac{x_i+x_{i+1}}{2}, \frac{y_j+y_{j+1}}{2})$ [49], [51], [70]. In this case, $f^* := f_{(0)}^* + \iota f_{(1)}^*$ satisfies $f^*(x, y) \neq 0$ for all $(x, y) \in \Omega$. Then we obtain θ_{f^*} by applying APU along a suitable path Υ , e.g.,

$$\Upsilon_1^{(x,y)}(\tau) := \begin{cases} (\tau, 0) & \text{if } 0 \leq \tau \leq x; \\ (x, \tau - x) & \text{if } x \leq \tau \leq x + y, \end{cases}$$

or

$$\Upsilon_2^{(x,y)}(\tau) := \begin{cases} (0, \tau) & \text{if } 0 \leq \tau \leq y; \\ (\tau - x, y) & \text{if } y \leq \tau \leq x + y. \end{cases}$$

The results along Υ_1 and Υ_2 are exactly the same and shown in Fig. 3(e). For each image in Fig. 3, the sample values in $[\text{Min}, \text{Max}]$ over \mathcal{G} are rescaled into $[0, 255]$ (black) to $[0, 255]$ (white).³

However, for estimation of Θ in Fig. 3(a), if Θ^W (Fig. 4(a)) is contaminated by more significant white Gaussian noise ($\sigma^2 = 1/4$) over \mathcal{R} , $f_{(0)}^* \in \mathcal{S}_4^2(\Delta_{\dagger})$ (Fig. 4(b)) and $f_{(1)}^* \in \mathcal{S}_4^2(\Delta_{\dagger})$ (Fig. 4(c)) computed by SPS have some common zeros. In this case, from Fact 2, θ_{f^*} is not well-defined in

³This rule of mapping is also employed in Figs. 4, 6, 8 and 10.

Ω . Actually, we see that θ_{f^*} computed by APU along Υ_1 (Fig. 4(d)) and Υ_2 (Fig. 4(e)) are very different, which is caused by the path dependency due to the common zeros. From this example, we find out that severe phase noise can create undesired common zeros of $f_{(0)}^*$ and $f_{(1)}^*$ in SPS. \square

D. Denoising by Selective Smoothing (DSS)

It is well-known that phase noise observed at even small portion of sampling points can create residues which influence the global feature of the results of existing 2D phase unwrapping algorithms (see, e.g., [1], [2], [43]–[45]). This has been a central reason of the difficulty in 2D phase unwrapping. In the proposed scheme for noisy wrapped samples, the occurrence of common zeros of $f_{(0)}^*$ and $f_{(1)}^*$ in SPS (or SPS+ or SPS++), which yields the path dependency of θ_{f^*} in APU (see Fig. 4), can be seen as such a type of difficulty. These facts suggest that excessive fidelity to noisy wrapped samples easily leads to poor estimates in 2D phase unwrapping problem.

In this subsection, to suppress the influence of noise, we denoise the wrapped phase $\Theta^W(x, y)$ ($(x, y) \in \mathcal{G}$) to obtain $\tilde{\Theta}^W(x, y) \in (-\pi, \pi]$ ($(x, y) \in \mathcal{G}' \supset \mathcal{G}$) by smoothing Θ^W while keeping the condition $\tilde{\Theta}^W(x, y) = \Theta^W(x, y)$ for all $(x, y) \in \mathcal{G}_I \subset \mathcal{G}$, where \mathcal{G}_I is the set of all reliable sampling points to be defined below. The reliability of each sampling point is judged on the basis of the wrapped phase difference. The smoothing is realized by using convex optimization. The main idea of *Denoising by Selective Smoothing (DSS)* is divided into the following two substeps.

DSS-1: Classify all sampling points in \mathcal{G} into \mathcal{G}_I (Type I: reliable) and $\mathcal{G}_{II} := \mathcal{G} \setminus \mathcal{G}_I$ (Type II: unreliable) on the basis of $W(\Delta\Theta_i^W)$ (see Section III-D-1).

DSS-2: Produce smoothed wrapped samples $\tilde{\Theta}^W(x, y) \in (-\pi, \pi]$ at $(x, y) \in \mathcal{G}' \supset \mathcal{G}$, where $\tilde{\Theta}^W$ satisfies

$$\tilde{\Theta}^W(x, y) = \Theta^W(x, y) \quad \text{if } (x, y) \in \mathcal{G}_I$$

and $\tilde{\Theta}^W(x, y)$ at $(x, y) \in \mathcal{G}' \setminus \mathcal{G}_I$ is determined by using convex optimization (see Section III-D-2) and interpolation (see Section III-D-3).

In what follows, for simplicity, assume that Θ^W is observed on $\mathcal{G} := \{(x_i, y_j)\}_{j=0,1,\dots,m}^{i=0,1,\dots,n}$ s.t. $x_i - x_{i-1} =: h_x > 0$ ($i = 1, 2, \dots, n$) and $y_j - y_{j-1} =: h_y > 0$ ($j = 1, 2, \dots, m$), and we use the notations $\Theta_{i,j} := \Theta(x_i, y_j)$, $\Theta_{i,j}^W := \Theta^W(x_i, y_j)$ and $\Theta := \text{vec}(\Theta_{i,j})_{j=0,1,\dots,m}^{i=0,1,\dots,n} \in \mathbb{R}^{(m+1)(n+1)}$.

1) *Classification of Sampling Points (DSS-1)*: In general, at sampling points where the unwrapped phase changes significantly, i.e., $|\Delta\Theta_i|$ is large, the variance of phase noise ν tends to become large (see, e.g., *maximum phase gradient maps* of InSAR and MRI examples in [1, Section 3.3.4]). Indeed, such noise model is widely employed, e.g., in [71]. This fact can also be explained in the scenario of InSAR terrain height estimation by inherent measurement error due to *geometric decorrelation* [72]–[74] which occurs at sampling points where the height changes significantly. Since the relation between the height difference ΔH_i and the unwrapped phase difference $\Delta\Theta_i$ can be explained from (26) (or (27)) in Section IV-A, large phase noise easily happens at sampling points where $|\Delta\Theta_i|$ is large. More seriously, large noise at such points often

creates residues (see (30) in Appendix A) which influence globally the results of 2D phase unwrapping [43]–[45].

From the above observation and the relation in (3), we use $W(\Delta\Theta_i^W)$ as a criterion to define $\mathcal{G}_I \subset \mathcal{G}$ and $\mathcal{G}_{II} := \mathcal{G} \setminus \mathcal{G}_I$. We assign $(x_i, y_j) \in \mathcal{G}$ to \mathcal{G}_I if

$$\forall (\tilde{x}, \tilde{y}) \in \mathcal{N}(x_i, y_j) \quad |W(\Theta^W(\tilde{x}, \tilde{y}) - \Theta^W(x_i, y_j))| \leq \kappa$$

and

$$(\tilde{r}_{i-1,j-1}, \tilde{r}_{i-1,j}, \tilde{r}_{i,j-1}, \tilde{r}_{i,j}) = (0, 0, 0, 0),$$

where $\mathcal{N}(x_i, y_j) \subset \mathcal{G}$ is the set of all neighboring sampling points of (x_i, y_j) , i.e., $\text{card}(\mathcal{N}(x_i, y_j)) \leq 4$, $\kappa \in [0, \pi]$ is a threshold⁴ and $\tilde{r}_{k,l} \in \{-1, 0, +1\}$ is defined as $\tilde{r}_{k,l} := r_{k,l}$ in (30) if $(k, l) \in [0, n-1] \times [0, m-1]$ and as $\tilde{r}_{k,l} := 0$ otherwise.⁵

2) *Convex Optimization for Smoothing (DSS-2a)*: In order to denoise unreliable wrapped samples $\Theta^W(x, y)$ ($(x, y) \in \mathcal{G}_{II}$), we first find a minimizer $\Theta_{(p)}^* := \text{vec}(\Theta_{(p)i,j}^*)_{j=0,1,\dots,m}^{i=0,1,\dots,n}$ of the following convex function:

$$\begin{aligned} \tilde{J}_\delta(\Theta) &:= \tilde{J}(\Theta) + \delta \|\Theta\|_2^2 \\ &:= \sum_{i=0}^{n-1} \sum_{j=0}^m w_{i,j}^x |\Theta_{i+1,j} - \Theta_{i,j} - W(\Theta_{i+1,j}^W - \Theta_{i,j}^W)| \\ &\quad + \sum_{i=0}^n \sum_{j=0}^{m-1} w_{i,j}^y |\Theta_{i,j+1} - \Theta_{i,j} - W(\Theta_{i,j+1}^W - \Theta_{i,j}^W)| \\ &\quad + \sum_{i=0}^{n-2} \sum_{j=0}^m w_{i,j}^{xx} |\Theta_{i+2,j} - 2\Theta_{i+1,j} + \Theta_{i,j}|^2 \\ &\quad + \sum_{i=0}^{n-1} \sum_{j=0}^{m-1} w_{i,j}^{xy} |\Theta_{i+1,j+1} - \Theta_{i+1,j} - \Theta_{i,j+1} + \Theta_{i,j}|^2 \\ &\quad + \sum_{i=0}^n \sum_{j=0}^{m-2} w_{i,j}^{yy} |\Theta_{i,j+2} - 2\Theta_{i,j+1} + \Theta_{i,j}|^2 + \delta \|\Theta\|_2^2, \end{aligned} \quad (20)$$

where $w_{i,j}^x$, $w_{i,j}^y$, $w_{i,j}^{xx}$, $w_{i,j}^{xy}$ and $w_{i,j}^{yy}$ are positive weights,⁶ and $\delta \|\Theta\|_2^2$ ($0 < \delta \ll 1$) is introduced for the regularization due to $\tilde{J}(\Theta) = \tilde{J}(\Theta + c(1, 1, \dots, 1)^T)$ for any $\Theta \in \mathbb{R}^{(m+1)(n+1)}$ and any $c \in \mathbb{R}$. \tilde{J} can be seen as a generalization of the cost employed in [34] (for ℓ_1), i.e., J in (32) in Appendix A-(III), by introducing an additional smoothness prior, the weighted ℓ_2 norm of the second order differences of Θ ,⁷ to J . The minimizer $\Theta_{(p)}^*$ is obtained by convex optimization techniques.⁸

The uncertainty of the minimizers of \tilde{J} is corrected by a translation as

$$\tilde{\Theta}_{(p)i,j}^* := \Theta_{(p)i,j}^* + \frac{1}{\text{card}(\mathcal{G}_I)} \sum_{(x_i, y_j) \in \mathcal{G}_I} W(\Theta_{i,j}^W - \Theta_{(p)i,j}^*)$$

⁴To keep a sufficient number of samples of Type I, we can design κ by using the histogram of $|W(\Delta\Theta_i^W)|$.

⁵For other useful criteria to judge the reliability, see, e.g., [1, Section 3.3].

⁶Note that $(w_{i,j}^x, w_{i,j}^y)$ are weights for data fidelity and $(w_{i,j}^{xx}, w_{i,j}^{xy}, w_{i,j}^{yy})$ are weights for smoothness. We can adjust the ratio of these two types of weights on the basis of geometric complexity of the target (see Section IV-B for targets of complex shape where relatively smaller magnitude is used for $(w_{i,j}^{xx}, w_{i,j}^{xy}, w_{i,j}^{yy})$ than that in Example 2 for a target of simple shape). Of course, if such geometric information on the target is available further in each local region, we can also adjust the ratio depending on (i, j) .

⁷In (20), we can also use other smoothness priors, e.g., *total variation* [75], [76], in place of the ℓ_2 norm of the second order differences.

⁸In Section III-E and Section IV-C, we use *alternating direction method of multipliers (ADMM)* [77]–[79] to minimize \tilde{J}_δ in (20).

Input: $\Theta^W(x, y)$ $((x, y) \in \mathcal{G})$, $\kappa \in [0, \pi]$ and $l \in \mathbb{Z}_{++}$

Output: θ_{f^*}

- 1: SPS/SPS+/SPS++ for $\Theta^W(x, y)$ $((x, y) \in \mathcal{G})$ (see Section III-B)
- 2: APU (see Section III-C)
- 3: **while** θ_{f^*} depends on the integration path **do**
- 4: Increase the weights $w_{i,j}^{xx}$, $w_{i,j}^{xy}$ and $w_{i,j}^{yy}$ for further smoothing
- 5: DSS for $\Theta^W(x, y)$ $((x, y) \in \mathcal{G})$ (see Section III-D)
- 6: SPS/SPS+/SPS++ for $\tilde{\Theta}^W(x, y)$ $((x, y) \in \mathcal{G}')$
- 7: APU
- 8: **end while**
- 9: Return θ_{f^*}

Fig. 5. Overall steps of the proposed 2D phase unwrapping scheme.

for improvement of the consistency with $\Theta_{i,j}^W$ at reliable sampling points $(x_i, y_j) \in \mathcal{G}_I$, where $\Theta_{(p)i,j}^* + W(\Theta_{i,j}^W - \Theta_{(p)i,j}^*)$ is the nearest phase in $\Theta_{i,j}^W + 2\pi\mathbb{Z}$ from $\Theta_{(p)i,j}^*$, i.e., $\Theta_{(p)i,j}^* + W(\Theta_{i,j}^W - \Theta_{(p)i,j}^*) = \arg\min_{\vartheta \text{ s.t. } W(\vartheta) = \Theta_{i,j}^W} |\vartheta - \Theta_{(p)i,j}^*|$.

3) *Denoised Wrapped Samples (DSS-2b)*: Set $l \in \mathbb{Z}_{++}$ on the basis of geometric complexity of the target, e.g., possible variation of terrain height, to be estimated in the applications of 2D phase unwrapping. Let $\mathcal{G}' := \{(x'_i, y'_j)\}_{j=0,1,\dots,lm}^{i=0,1,\dots,ln}$ s.t. $x'_0 = x_0$, $x'_{ln} = x_n$, $y'_0 = y_0$, $y'_{lm} = y_m$, $x'_i - x'_{i-1} = h_x/l$ ($i = 1, 2, \dots, ln$), and $y'_j - y'_{j-1} = h_y/l$ ($j = 1, 2, \dots, lm$). The wrapped phase over \mathcal{G}' after denoising is obtained as

$$\tilde{\Theta}^W(x, y) := \begin{cases} \Theta^W(x, y) & \text{if } (x, y) \in \mathcal{G}_I; \\ W(\text{BLI}[\tilde{\Theta}_{(p)}^*](x, y)) & \text{if } (x, y) \in \mathcal{G}' \setminus \mathcal{G}_I, \end{cases} \quad (21)$$

where $\text{BLI}[\tilde{\Theta}_{(p)}^*] : \Omega \rightarrow \mathbb{R}$ stands for the bilinear interpolation of $\tilde{\Theta}_{(p)}^* := \text{vec}(\tilde{\Theta}_{(p)i,j}^*)_{j=0,1,\dots,m}^{i=0,1,\dots,n}$.

Remark 3 (On the Utilization of DSS): We combine DSS with SPS (or SPS+ or SPS++) and APU as follows.

- (i) From (21), DSS does not influence at all given wrapped phase $\Theta^W(x, y)$ at $(x, y) \in \mathcal{G}_I$. If application of SPS or SPS+ with $\epsilon_{(k)}(x, y) = 0$ ($(x, y) \in \mathcal{G}_I$ and $k = 0, 1$) to $\tilde{\Theta}^W(x, y)$ ($(x, y) \in \mathcal{G}'$) yields $f^* = f_{(0)}^* + \iota f_{(1)}^*$ having no zero in Ω , then we can guarantee

$$W(\theta_{f^*}(x, y)) = \Theta^W(x, y) \quad \text{for all } (x, y) \in \mathcal{G}_I. \quad (22)$$

We also remark that it is reasonable to use $\epsilon_{(k)}(x, y) > 0$ ($(x, y) \in \mathcal{G}' \setminus \mathcal{G}_I$) in SPS+ because $\tilde{\Theta}^W(x, y)$ is influenced by smoothing effect of DSS and $\mathcal{G}_{II} \subset \mathcal{G}' \setminus \mathcal{G}_I$.

- (ii) If f^* computed by SPS (or SPS+ or SPS++) for $\tilde{\Theta}^W$ has zeros in Ω , the path independency of θ_{f^*} and relation (22) are not guaranteed in APU. In such a case, we repeat DSS after increasing the weights $w_{i,j}^{xx}$, $w_{i,j}^{xy}$ and $w_{i,j}^{yy}$ in (20) for further smoothing (see Fig. 5 in Section III-E). \square

E. Overall Steps of the Proposed Scheme

Given wrapped samples $\Theta^W(x, y)$ $((x, y) \in \mathcal{G})$, the overall steps of the proposed 2D phase unwrapping scheme is finally summarized in Fig. 5. Note that SPS (or SPS+ or SPS++) APU and DSS yield a smooth continuous phase function θ_{f^*} , as a high-resolution estimate of Θ , which is consistent with the wrapped phase at reliable sampling points, i.e., $W(\theta_{f^*}(x, y)) = \Theta^W(x, y)$ at $(x, y) \in \mathcal{G}_I$ (see Example 2).

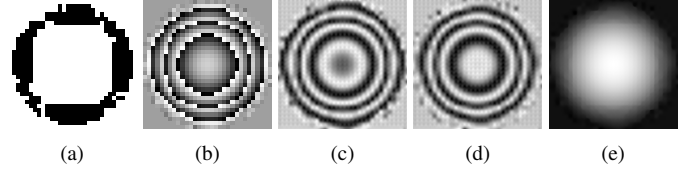


Fig. 6. Numerical example of the proposed 2D phase unwrapping (DSS, SPS+ and APU): (a) distribution of Type I (white) and Type II (black) samples, (b) $\tilde{\Theta}^W$ by DSS, (c) $f_{(0)}^*$ by SPS+, (d) $f_{(1)}^*$ by SPS+, and (e) θ_{f^*} by APU.

Example 2 (2D Phase Unwrapping by DSS, SPS+ and APU):

According to the proposed scheme in Fig. 5, we apply the denoising step DSS to Θ^W in Fig. 4(a) for which SPS and APU failed in unwrapping as shown in Figs. 4(d) and 4(e). We set $\kappa = 2\pi/3$, $w_{i,j}^x = w_{i,j}^y = w_{i,j}^x = w_{i,j}^{xy} = w_{i,j}^{yy} = 1$, $\delta = 5 \times 10^{-7}$, and $l = 1$, i.e., $\mathcal{G}' = \mathcal{G}$, for DSS. Figures 6(a) and 6(b) respectively show the distribution of samples of Type I & Type II and the denoised wrapped phase $\tilde{\Theta}^W$ by DSS from which we see that $\tilde{\Theta}^W$ is certainly smoother than Θ^W around \mathcal{R} . Figures 6(c) and 6(d) respectively show $f_{(0)}^* \in \mathcal{S}_4^2(\Delta_{\dagger})$ and $f_{(1)}^* \in \mathcal{S}_4^2(\Delta_{\dagger})$ obtained by applying SPS+ to $\tilde{\Theta}^W$, where we set $\epsilon_{(0)}(x, y) = \epsilon_{(1)}(x, y) = 0$ if $(x, y) \in \mathcal{G}_I$ to guarantee (22), and set $\epsilon_{(0)}(x, y) = 0.5 - 0.5|\cos(\tilde{\Theta}^W(x, y))|$ and $\epsilon_{(1)}(x, y) = 0.5 - 0.5|\sin(\tilde{\Theta}^W(x, y))|$ otherwise. In this case, $f_{(0)}^*$ and $f_{(1)}^*$ have no common zero over Ω . Hence, by applying APU along any suitable path Υ , we can obtain θ_{f^*} in Fig. 6(e) satisfying $W(\theta_{f^*}(x, y)) = \Theta^W(x, y)$ for all $(x, y) \in \mathcal{G}_I$. \square

IV. APPLICATION TO TERRAIN HEIGHT ESTIMATION

In this section, we apply the proposed 2D phase unwrapping scheme to InSAR terrain height estimation.

A. Terrain Height Estimation by InSAR

Interferometric synthetic aperture radar (InSAR) [3]–[9] is an imaging technique allowing highly accurate measurements of surface topography in all weather conditions, day or night. In InSAR system (see Fig. 7(a)), Antenna 1 and Antenna 2 on-board an aircraft or a spacecraft platform transmit coherent broadband radio signals and receive the reflected signals $s_k := |s_k|e^{-\iota(\frac{4\pi R_k}{\lambda} + \phi_k + \nu_k)}$ ($k = 1, 2$) from a target corresponding to $(x, y) \in \Omega$, where λ is the wavelength of the transmitted signal, R_k is the distance from Antenna k to the target, ϕ_k is the backscatter phase delay, ν_k is additive phase noise, and the dependencies of variables R_k , ϕ_k , ν_k , θ_o and θ_i on (x, y) are omitted for notational simplicity in Fig. 7 and in the discussion below. Since the backscatter phase delay ϕ_k is determined by the shape of the target, geological condition, and weather condition, we can expect $\phi_1 = \phi_2$ in many situations, and hence the interferometric image is obtained as

$$\bar{s}_1 s_2 = |s_1| |s_2| e^{\iota(\frac{4\pi(R_1 - R_2)}{\lambda} + \nu)}, \quad (23)$$

where \bar{s}_1 denotes the complex conjugate of s_1 and $\nu := \nu_1 - \nu_2$. The *interferometric phase* $\Theta_{\text{int}}(x, y) := 4\pi(R_1 - R_2)/\lambda$ can also be expressed, from the simple geometric relation in Fig. 7(a) and the law of cosines, as

$$\Theta_{\text{int}}(x, y) = \frac{4\pi}{\lambda} \left(R_1 - \sqrt{R_1^2 + B^2 - 2R_1 B \sin(\theta_o - \alpha)} \right), \quad (24)$$

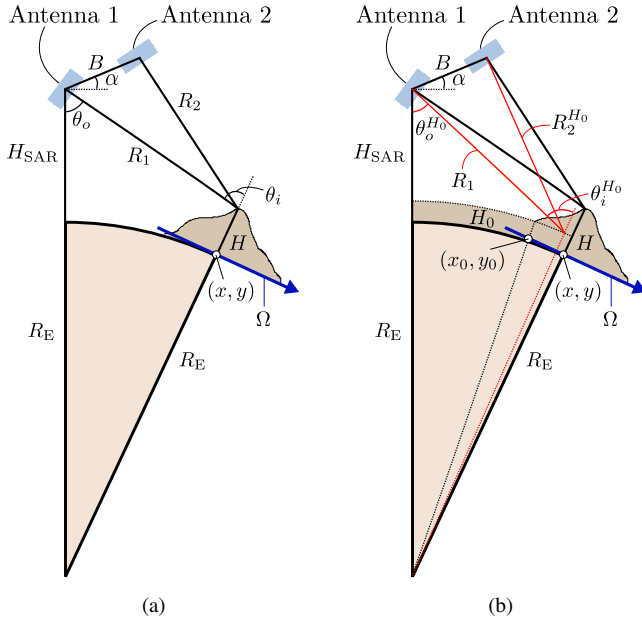


Fig. 7. InSAR imaging geometry for terrain height estimation: (a) sectional view to define the interferometric phase $\Theta_{\text{int}}(x, y)$ in (24) and (b) sectional view to define the reference phase $\Theta_{\text{ref}}(x, y)$ in (25).

and its noisy wrapped samples $\Theta_{\text{int}}^W(x, y) := W(\Theta_{\text{int}}(x, y) + \nu(x, y))$ are observed from (23). The terrain height H at $(x, y) \in \Omega$ is expressed by

$$H(x, y) = \sqrt{(H_{\text{SAR}} + R_E - R_1 \cos \theta_o)^2 + R_1^2 \sin^2 \theta_o} - R_E$$

as shown in [6], or by

$$H(x, y) = (H_{\text{SAR}} + R_E) \cos(\theta_i - \theta_o) - R_E - R_1 \cos \theta_i,$$

where H_{SAR} is the height of Antenna 1, R_E is the radius of the earth, and the incidence angle θ_i is given, with the use of the off-nadir angle θ_o by $\theta_i = \arctan\left(\frac{(H_{\text{SAR}} + R_E) \sin \theta_o}{(H_{\text{SAR}} + R_E) \cos \theta_o - R_1}\right)$. Hence, by reconstructing Θ_{int} from the noisy wrapped phase Θ_{int}^W , we can compute θ_o , θ_i and H if α , B , R_1 , R_E , and H_{SAR} are available (Note: More precisely, for reconstruction of Θ_{int} , we also need the absolute interferometric phase at some point $(x_0, y_0) \in \Omega$ where the height $H(x_0, y_0)$ is known). However, the available measurements of R_1 , R_E , and H_{SAR} contain errors and directly degrade estimation accuracy of H through the above equations. To suppress the degradation, H is estimated as follows [73]. Suppose that we know the terrain height at $(x_0, y_0) \in \Omega$ is $H(x_0, y_0) = H_0$ (see Fig. 7(b)). Let

$$\begin{aligned} \Theta_{\text{ref}}(x, y) &:= \frac{4\pi(R_1 - R_2^{H_0})}{\lambda} \\ &= \frac{4\pi}{\lambda} \left(R_1 - \sqrt{R_1^2 + B^2 - 2R_1 B \sin(\theta_o^{H_0} - \alpha)} \right), \end{aligned} \quad (25)$$

where $R_2^{H_0}$ and $\theta_o^{H_0}$ at $(x, y) \in \Omega$, indicated in Fig. 7(b), are available from $\cos \theta_o^{H_0} = \frac{R_1^2 + (R_E + H_{\text{SAR}})^2 - (R_E + H_0)^2}{2R_1(R_E + H_{\text{SAR}})}$. Θ_{ref} is called the *reference phase* and the following 2D phase function $\Theta(x, y) := \Theta_{\text{int}}(x, y) - \Theta_{\text{ref}}(x, y)$ is known to be more reliable to use for estimation of H than Θ_{int} . Actually, Θ is more robust than Θ_{int} against the measurement errors in R_1 , R_E and H_{SAR} while the sensitivities of Θ and Θ_{int} to H

are identical, which is confirmed by

$$\left. \begin{aligned} \frac{\partial \Theta}{\partial R_1} &= \frac{\partial \Theta_{\text{int}}}{\partial R_1} - \frac{\partial \Theta_{\text{ref}}}{\partial R_1} \approx 0 \\ \frac{\partial \Theta}{\partial R_E} &= \frac{\partial \Theta_{\text{int}}}{\partial R_E} - \frac{\partial \Theta_{\text{ref}}}{\partial R_E} \approx 0 \\ \frac{\partial \Theta}{\partial H_{\text{SAR}}} &= \frac{\partial \Theta_{\text{int}}}{\partial H_{\text{SAR}}} - \frac{\partial \Theta_{\text{ref}}}{\partial H_{\text{SAR}}} \approx 0 \end{aligned} \right\}$$

and

$$\frac{\partial \Theta}{\partial H} = \frac{\partial \Theta_{\text{int}}}{\partial H} = \frac{4\pi B \cos(\theta_o - \alpha)}{\lambda \sin \theta_i \sqrt{R_1^2 + B^2 - 2R_1 B \sin(\theta_o - \alpha)}}. \quad (26)$$

The expression (26) can be approximated as

$$\frac{\partial \Theta}{\partial H} \approx \frac{4\pi B \cos(\theta_o - \alpha)}{\lambda \sin \theta_i R_1}, \quad (27)$$

which is found, e.g., in [72]–[74] (see Appendix E).

To estimate $H(x, y)$, we also use

$$\Theta(x, y) \approx \frac{4\pi B \cos(\theta_o^{H_0} - \alpha)(H(x, y) - H_0)}{\lambda \sin \theta_i^{H_0} \sqrt{R_1^2 + B^2 - 2R_1 B \sin(\theta_o^{H_0} - \alpha)}} \quad (28)$$

as a refinement of [80, Equation (A.2.7)] (see Appendix E), where $\theta_i^{H_0}$, indicated in Fig. 7(b), is available from $\sin \theta_i^{H_0} = \frac{(R_E + H_{\text{SAR}}) \sin \theta_o^{H_0}}{R_E + H_0}$. The noisy wrapped phase $\Theta^W(x, y) := W(\Theta_{\text{int}}(x, y) - \Theta_{\text{ref}}(x, y) + \nu(x, y)) = W(\Theta_{\text{int}}^W(x, y) - \Theta_{\text{ref}}(x, y))$ is obtained from (23) and Θ_{ref} . After reconstructing Θ from Θ^W , H is estimated from (28).

B. Parameter Settings of the Proposed Scheme

Assume that noisy wrapped samples $\Theta^W(x, y)$ are observed on regular rectangular grid points $\mathcal{G} := \{(x_i, y_j)\}_{j=0,1,\dots,m}^{i=0,1,\dots,n}$ s.t. $x_i - x_{i-1} =: h_x > 0$ ($i = 1, 2, \dots, n$) and $y_j - y_{j-1} =: h_y > 0$ ($j = 1, 2, \dots, m$) in $\Omega := [x_0, x_n] \times [y_0, y_m]$.

In DSS, the denoised wrapped samples $\tilde{\Theta}^W(x, y)$ on $\mathcal{G}' := \{(x'_i, y'_j)\}_{j=0,1,\dots,lm}^{i=0,1,\dots,ln}$ are obtained by $\kappa = \pi/4$, $l = 3$, $w_{i,j}^x = w_{i,j}^y = 1$, $w_{i,j}^{xx} = w_{i,j}^{yy} = w_{i,j}^{xy} = 1/100$ and $\delta = 5 \times 10^{-7}$ (see Section III-D and Footnotes 4 & 6 for basic ideas on parameter settings, and see also Figs. 8(g) & 10(g) for the effect of κ).

After DSS, we use SPS+ to obtain the smoothest spline functions $f_{(k)}^* \in \mathcal{S}_4^2(\Delta_{\dagger})$ ($k = 0, 1$), where Δ_{\dagger} is a crisscross partition by cutting every rectangle $[x'_i, x'_{i+1}] \times [y'_j, y'_{j+1}]$ into four triangles as introduced in Example 1. In SPS+, we set $\epsilon_{(0)}(x, y) = \epsilon_{(1)}(x, y) = 0$ if $(x, y) \in \mathcal{G}_1$ to guarantee (22), and set $\epsilon_{(0)}(x, y) = 0.5 - 0.5|\cos(\tilde{\Theta}^W(x, y))|$ and $\epsilon_{(1)}(x, y) = 0.5 - 0.5|\sin(\tilde{\Theta}^W(x, y))|$ otherwise (see Remark 3(i)).

In APU, we use the idea in Appendix D for a fast and stable computation of $V(\Psi(\tau^*))$ and $V(\Psi(a))$ in (19).

C. Numerical Experiments

We demonstrate the effectiveness of the proposed 2D phase unwrapping scheme by terrain height estimation based on (28). Figure 8(a) shows the unwrapped phase Θ generated from a test mountain shown in Fig. 9(a). Here we set the parameters of InSAR system by $\alpha = \pi/6$ [rad], $\lambda = 23.5$ [cm], $B = 500$ [m], $H_{\text{SAR}} = 800$ [km], $R_E = 6371$ [km], $R_1(x_0, y_0) = 1243$ [km], and $H(x_0, y_0) = H_0 = 2530$ [m]. Figure 8(b)

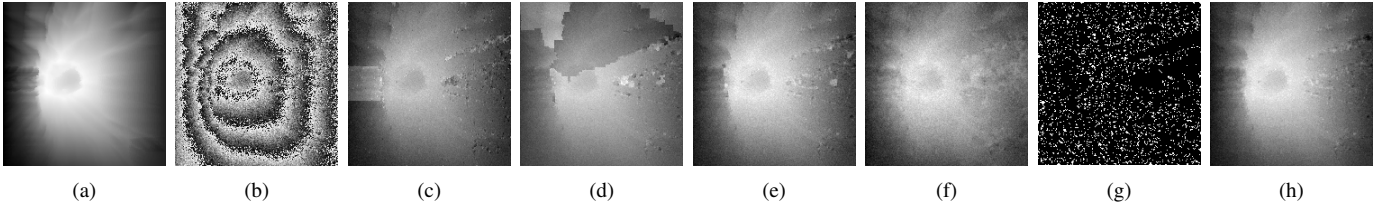


Fig. 8. Comparison of the proposed 2D phase unwrapping and the existing 2D phase unwrapping (I): (a) unwrapped phase Θ (to be estimated), (b) wrapped phase Θ^W , (c) estimate by BC (MSE = 1.7587), (d) estimate by MST (MSE = 8.2192), (e) estimate by MCF (MSE = 0.0974), (f) estimate by MLN (MSE = 20.4673), (g) distribution of Type I (white) and Type II (black), and (h) estimate by the proposed scheme (DSS, SPS+ and APU) (MSE = 0.0379), where MSE is the mean square error of each estimate, i.e., $\text{MSE} := \frac{1}{32761} \sum_{i=0}^{180} \sum_{j=0}^{180} |\Theta_{i,j} - \Theta_{i,j}^*|^2$ (Θ^* : estimate).

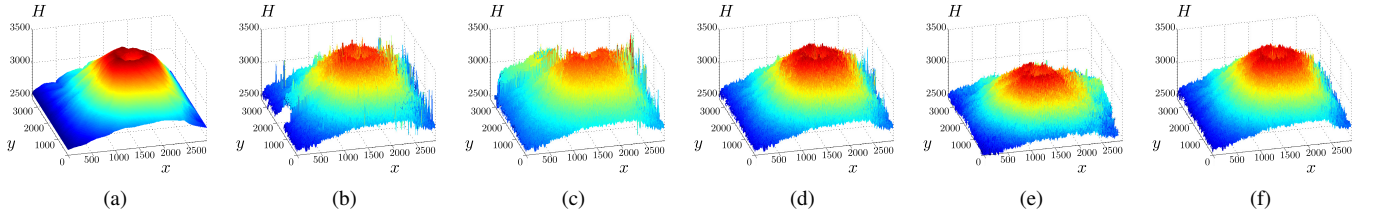


Fig. 9. Comparison of terrain height estimations based on the proposed 2D phase unwrapping and the existing 2D phase unwrapping (I): (a) test mountain of height H (to be estimated), (b) estimate by BC (MAE = 37.6844), (c) estimate by MST (MAE = 87.1949), (d) estimate by MCF (MAE = 26.9321), (e) estimate by MLN (MAE = 162.3990), and (f) estimate by the proposed scheme (DSS, SPS+ and APU) (MAE = 23.2882), where MAE is the mean absolute error of each estimate, i.e., $\text{MAE} := \frac{1}{32761} \sum_{i=0}^{180} \sum_{j=0}^{180} |H_{i,j} - H_{i,j}^*|$ (H^* : estimate).

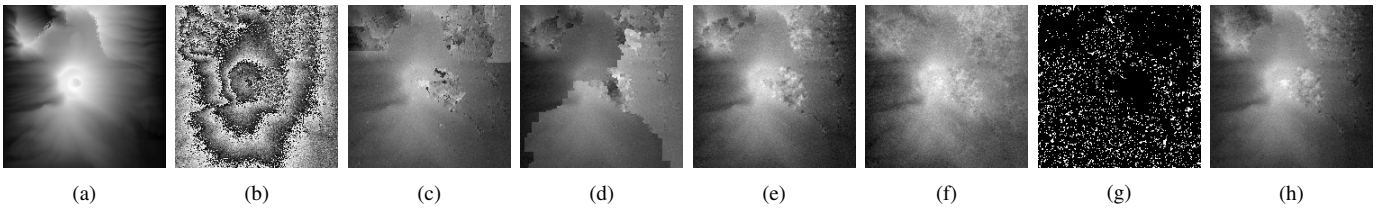


Fig. 10. Comparison of the proposed 2D phase unwrapping and the existing 2D phase unwrapping (II): (a) unwrapped phase Θ (to be estimated), (b) wrapped phase Θ^W , (c) estimate by BC (MSE = 2.5410), (d) estimate by MST (MSE = 49.4547), (e) estimate by MCF (MSE = 1.4087), (f) estimate by MLN (MSE = 5.8364), (g) distribution of Type I (white) and Type II (black), and (h) estimate by the proposed scheme (DSS, SPS+ and APU) (MSE = 0.2011).

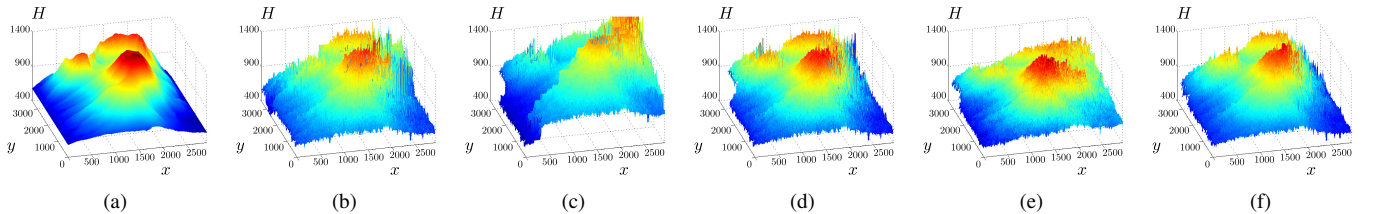


Fig. 11. Comparison of terrain height estimations based on the proposed 2D phase unwrapping and the existing 2D phase unwrapping (II): (a) test mountain of height H (to be estimated), (b) estimate by BC (MAE = 52.1210), (c) estimate by MST (MAE = 210.7460), (d) estimate by MCF (MAE = 41.1130), (e) estimate by MLN (MAE = 86.7128), and (f) estimate by the proposed scheme (DSS, SPS+ and APU) (MAE = 30.3923).

depicts the wrapped phase Θ^W on $\mathcal{G} := \{(x_i, y_j)\}_{j=0,1,\dots,180}^{i=0,1,\dots,180}$ s.t. $h_x = 16.2$ [m] and $h_y = 19.5$ [m], where additive phase noise ν is generated by [71]. Figures 8(c), 8(d), 8(e), and 8(f) respectively depict the estimates of Θ by *branch cut* (BC) [5], *minimum spanning tree* (MST) [26], *minimum cost flow* (MCF) [29] (all weights are '1'), and *minimum ℓ_p norm* (MLN) [34] ($p = 2$ and all weights are '1') (see Appendix A). Figure 8(g) shows the distribution of samples of Type I and Type II from which we see that samples of Type I distribute sparsely but almost uniformly over Ω . Figure 8(h) depicts the estimate of Θ by the proposed scheme (DSS, SPS+ and APU). Figures 9(b), 9(c), 9(d), 9(e), and 9(f) show the mountains constructed from the results in Fig. 8 and (28). Figures 8 and 9 show that the proposed scheme achieves the best performance compared with the other algorithms visually as well as numerically.

Figure 10(a) shows the unwrapped phase Θ generated from another test mountain in Fig. 11(a). The parameter settings of InSAR system, the proposed scheme, and the other algorithms are the same as those used in the first simulation except for $R_1(x_0, y_0) = 1244$ [km] and $H(x_0, y_0) = H_0 = 579$ [m]. Figure 10(b) depicts the noisy wrapped phase Θ^W on $\mathcal{G} := \{(x_i, y_j)\}_{j=0,1,\dots,180}^{i=0,1,\dots,180}$. Figures 10(c), 10(d), 10(e), and 10(f) respectively depict the estimates of Θ by BC, MST, MCF, and MLN. Figure 10(g) shows the distribution of samples of Type I and Type II from which we see that samples of Type I of this example also distribute sparsely but almost uniformly over Ω . Figure 10(h) depicts the estimate by the proposed scheme (DSS, SPS+ and APU). Figures 11(b), 11(c), 11(d), 11(e), and 11(f) show the mountains based on the results in Fig. 10 and (28). In this example, the proposed 2D phase unwrapping

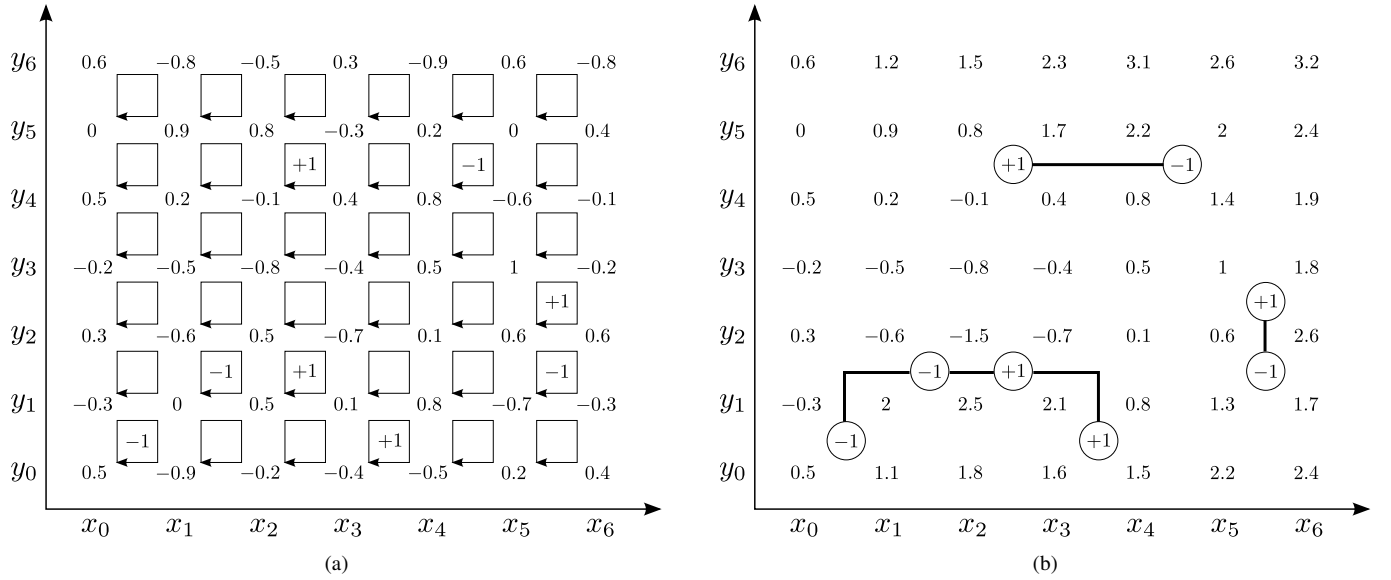


Fig. 12. Illustration of the basic idea of the network flow methods for 2D phase unwrapping: (a) detection of every closed loop $L_{i,j}$ having a residue $r_{i,j} = \pm 1$ in (30) based on given normalized wrapped phase $\Theta_{i,j}^W/\pi$ ($i = 0, 1, \dots, 6$ and $j = 0, 1, \dots, 6$) and (b) construction of the set of branches \mathcal{B} and an estimate $\Theta_{i,j}(E)/\pi$ ($i = 0, 1, \dots, 6$ and $j = 0, 1, \dots, 6$), where $E = E_x \cup E_y$, $E_x = \{((x_0, y_1), (x_1, y_1)), ((x_3, y_1), (x_4, y_1)), ((x_5, y_2), (x_6, y_2))\}$ and $E_y = \{((x_1, y_1), (x_1, y_2)), ((x_2, y_1), (x_2, y_2)), ((x_3, y_1), (x_3, y_2)), ((x_3, y_4), (x_3, y_5)), ((x_4, y_4), (x_4, y_5))\}$.

scheme achieves again the best performance compared with the other algorithms.

V. CONCLUSION

In this paper, we have proposed a novel 2D phase unwrapping scheme which is composed of SPS (or SPS+ or SPS++), APU and DSS. SPS (or SPS+ or SPS++) constructs a pair of the smoothest spline functions which minimize the energies of their local changes while satisfying respectively the desired data fidelity conditions specified with the cosine and the sine of given wrapped samples. If these functions have no common zero over the domain of interest, the proposed estimate of the unwrapped phase is computed by algebraic phase unwrapping (APU) as a continuous function defined over the domain. To avoid the occurrence of common zeros in SPS (or SPS+ or SPS++) due to phase noise, we also proposed a denoising step (DSS), as preprocessing, which selectively smooths unreliable wrapped samples by using convex optimization. The smoothness of the proposed estimate is guaranteed globally over the domain without losing any desired consistency with all reliable wrapped samples. Numerical experiments for InSAR terrain height estimation demonstrated the effectiveness of the proposed 2D phase unwrapping scheme.

APPENDIX A

EXISTING 2D PHASE UNWRAPPING ALGORITHMS

In this section, for simplicity, assume that noisy wrapped samples are observed on $\mathcal{G} := \{(x_i, y_j)\}_{j=0,1,\dots,m}^{i=0,1,\dots,n}$ in $\Omega := [x_0, x_n] \times [y_0, y_m]$ s.t. $x_0 < x_1 < \dots < x_n$ and $y_0 < y_1 < \dots < y_m$, and we use the notations $\Theta_{i,j} := \Theta(x_i, y_j)$, $\Theta_{i,j}^W := \Theta^W(x_i, y_j)$ and $\Theta := \text{vec}(\Theta_{i,j})_{j=0,1,\dots,m}^{i=0,1,\dots,n} \in \mathbb{R}^{(m+1)(n+1)}$.

Network flow methods [5], [25]–[30] try to find a minimizer of (2) under condition (4). For solving this combinatorial optimization problem, the network flow methods first detect every

closed loop $L_{i,j} := ((x_i, y_j) \rightarrow (x_i, y_{j+1}) \rightarrow (x_{i+1}, y_{j+1}) \rightarrow (x_{i+1}, y_j) \rightarrow (x_i, y_j))$ in \mathcal{G} satisfying

$$W(\Theta_{i,j+1}^W - \Theta_{i,j}^W) + W(\Theta_{i+1,j+1}^W - \Theta_{i,j+1}^W) \neq W(\Theta_{i+1,j}^W - \Theta_{i,j}^W) + W(\Theta_{i+1,j+1}^W - \Theta_{i+1,j}^W). \quad (29)$$

Such a closed loop $L_{i,j}$ is said to have a *residue*, and must pass at least one neighboring pair i s.t. $\Delta\Theta_i \neq W(\Delta\Theta_i^W)$ because otherwise

$$\begin{aligned} W(\Theta_{i,j+1}^W - \Theta_{i,j}^W) + W(\Theta_{i+1,j+1}^W - \Theta_{i,j+1}^W) &= (\Theta_{i,j+1} - \Theta_{i,j}) + (\Theta_{i+1,j+1} - \Theta_{i,j+1}) \\ &= (\Theta_{i+1,j} - \Theta_{i,j}) + (\Theta_{i+1,j+1} - \Theta_{i+1,j}) \\ &= W(\Theta_{i+1,j}^W - \Theta_{i,j}^W) + W(\Theta_{i+1,j+1}^W - \Theta_{i+1,j}^W) \end{aligned}$$

contradicts (29). The all closed loops $L_{i,j}$ ($i = 0, 1, \dots, n-1$ and $j = 0, 1, \dots, m-1$) are classified into three classes by discretized contour integrals:

$$\begin{aligned} r_{i,j} &:= \frac{1}{2\pi} \left(W(\Theta_{i,j+1}^W - \Theta_{i,j}^W) + W(\Theta_{i+1,j+1}^W - \Theta_{i,j+1}^W) \right. \\ &\quad \left. - W(\Theta_{i+1,j+1}^W - \Theta_{i+1,j}^W) - W(\Theta_{i+1,j}^W - \Theta_{i,j}^W) \right) \\ &= \begin{cases} 0 & (L_{i,j} \text{ has no residue}); \\ +1 & (L_{i,j} \text{ has a positive residue}); \\ -1 & (L_{i,j} \text{ has a negative residue}). \end{cases} \quad (30) \end{aligned}$$

After identifying the residues (see Fig. 12(a)), the network flow methods create the set of *branches* \mathcal{B} . Each branch is defined as a path connecting the positive and negative residues of the same number (see Fig. 12(b) and [5], [25]–[30]). If we define $E := E_x \cup E_y$ in Section I by

$$E_x := \left\{ \begin{array}{l} ((x_i, y_j), (x_{i+1}, y_j)) \\ \in \mathcal{G} \times \mathcal{G} \end{array} \left| \begin{array}{l} (x_i, y_j) \text{ and } (x_{i+1}, y_j) \\ \text{lie on the left and right} \\ \text{sides of some branch in } \mathcal{B} \end{array} \right. \right\}$$

and

$$E_y := \left\{ \begin{array}{l} ((x_i, y_j), (x_i, y_{j+1})) \\ \in \mathcal{G} \times \mathcal{G} \end{array} \left| \begin{array}{l} (x_i, y_j) \text{ and } (x_i, y_{j+1}) \\ \text{lie on the lower and upper} \\ \text{sides of some branch in } \mathcal{B} \end{array} \right. \right\},$$

we can construct a candidate of the unwrapped phase $\Theta(E) := \text{vec}(\Theta_{i,j}(E))_{j=0,1,\dots,n}^{i=0,1,\dots,m}$ satisfying condition (4), $\Delta\Theta_i(E) = W(\Delta\Theta_i^W)$ if $i \notin E$, and $\Delta\Theta_i(E) \neq W(\Delta\Theta_i^W)$ if $i \in E$ as shown in Fig. 12(b).

Assume for simplicity that J_i in (2) is designed to achieve 0 if $\Delta\Theta_i = W(\Delta\Theta_i^W)$. Then (5) can be expressed as

$$\widehat{J}(E) = \sum_{i \in E} J_i(\Delta\Theta_i(E)). \quad (31)$$

The network flow methods try to find optimal E^* (or equivalently optimal branches \mathcal{B}^*) minimizing (31). In the following, we introduce three major types of phase unwrapping algorithms, i.e., (I) *branch cut* [5] & *minimum spanning tree* [26], (II) *minimum cost flow* [29], which are examples of network flow methods, and (III) *minimum ℓ_p norm* [34], which is not classified into network flow methods and directly approximates a minimizer of (2) without requiring condition (4).

(I). Branch Cut and Minimum Spanning Tree

Branch cut (BC) algorithm was established by Goldstein et al. [5] and minimum spanning tree (MST) algorithm was established by Chen and Zebker [26]. These algorithms try to minimize (31), where the ℓ_0 (pseudo-)norm $\|\text{vec}(\Delta\Theta_i(E) - W(\Delta\Theta_i^W))_{i \in E}\|_0 = \text{card}(E)$ is employed as the cost \widehat{J} . Unfortunately, this optimization problem is NP-hard [26]. The BC algorithm is a heuristic algorithm designed to approximate \mathcal{B}^* by connecting the nearest residues repeatedly without checking whether the residues have been already connected with other residues. Therefore the same residues are connected many times, which makes many extra branches and results in poor estimates in region having many residues [26]. To overcome this shortcomings, the MST algorithm approximates \mathcal{B}^* by eliminating extra branches from the minimum spanning tree which connects all residues. Since the length of the spanning tree is an upper bound of $\text{card}(E)$, the MST algorithm approximates \mathcal{B}^* by using a minimizer of the upper bound.

(II). Minimum Cost Flow

Minimum cost flow (MCF) algorithm was established by Costantini [29]. The goal of the MCF algorithm is to minimize (31), where the weighted ℓ_1 norm $\|\text{vec}(\Delta\Theta_i(E) - W(\Delta\Theta_i^W))_{i \in E}\|_{1,w}$ is employed as \widehat{J} . It is shown [29] that this optimization problem can be interpreted as a *minimum cost integer-flow problem* by considering positive and negative residues as *supply* and *demand* nodes, respectively. Therefore E^* is computed by using minimum cost flow solvers [81].

(III). Minimum ℓ_p Norm

Minimum ℓ_p norm (MLN) algorithm was established by Ghiglia and Romero [34] as a generalized version of minimum ℓ_2 norm algorithm (the so-called *least squares method*) [31], [32]. Differently from network flow methods, the MLN algo-

rithm directly approximates $\Theta^* \in \mathbb{R}^{(m+1)(n+1)}$ minimizing

$$J(\Theta) = \sum_{i=0}^{n-1} \sum_{j=0}^m w_{i,j}^x |\Theta_{i+1,j} - \Theta_{i,j} - W(\Theta_{i+1,j}^W - \Theta_{i,j}^W)|^p + \sum_{i=0}^n \sum_{j=0}^{m-1} w_{i,j}^y |\Theta_{i,j+1} - \Theta_{i,j} - W(\Theta_{i,j+1}^W - \Theta_{i,j}^W)|^p \quad (32)$$

without requiring condition (4), where $w_{i,j}^x > 0$, $w_{i,j}^y > 0$ and $p > 0$. If $p \geq 1$, J is convex and we can obtain a minimizer Θ^* by convex optimization techniques. Note that as seen from $J(\Theta) = J(\Theta + c(1, 1, \dots, 1)^T)$ for any $\Theta \in \mathbb{R}^{(m+1)(n+1)}$ and any $c \in \mathbb{R}$, the minimizer is not uniquely determined.

APPENDIX B

OPTIMALITY OF SPLINE FUNCTIONS

For a given 1D data $\{(x_i, z_i)\}_{i=0}^n$ s.t. $a := x_0 < x_1 < \dots < x_n =: b$, it is well-known that there exists a unique solution, say $f^* \in C^2(\mathbb{R})$, of the following variational problem:

$$\min_{f \in C^2(\mathbb{R})} \int_a^b |f''(x)|^2 dx \quad \text{s.t. } f(x_i) = z_i \quad (i = 0, \dots, n),$$

and f^* is a *natural cubic spline* [54] which is a kind of univariate spline function of degree 3. This fact also guarantees that the solutions, if they exist, of the following variational problems:

$$\min_{f \in C^2(\mathbb{R})} \int_a^b |f''(x)|^2 dx \quad \text{s.t. } |f(x_i) - z_i| \leq \epsilon_i \quad (i = 0, \dots, n)$$

and

$$\min_{f \in C^2(\mathbb{R})} \sum_{i=0}^n |f(x_i) - z_i|^p + \lambda \int_a^b |f''(x)|^2 dx$$

are also natural cubic splines, where $\epsilon_i \geq 0$, $p > 0$, and the smoothing parameter $\lambda > 0$ controls the trade-off between data fidelity and smoothness (see [37] for the case of $p = 2$). This is because if there exists any solution g not a natural cubic spline, then we can construct a natural cubic spline $f \in C^2(\mathbb{R})$ satisfying $f(x_i) = g(x_i)$ ($i = 0, 1, \dots, n$) and $\int_a^b |f''(x)|^2 dx < \int_a^b |g''(x)|^2 dx$, which is absurd.

Certain 2D extensions of the above discussion are found, e.g., in [55], [56].

APPENDIX C

QUADRATIC FORM FOR ENERGY OF LOCAL CHANGE

Let $\Delta := \{\mathcal{T}_l\}_{l=1}^N$ be a regular triangulation s.t. $\bigcup_{l=1}^N \mathcal{T}_l =: \Omega$. The energy of local change of $f \in \mathcal{S}_d^q(\Delta)$ is defined as

$$\begin{aligned} & \iint_{\Omega} \left[\left| \frac{\partial^2 f}{\partial x^2} \right|^2 + 2 \left| \frac{\partial^2 f}{\partial x \partial y} \right|^2 + \left| \frac{\partial^2 f}{\partial y^2} \right|^2 \right] dx dy \\ &= \sum_{l=1}^N \iint_{\mathcal{T}_l} \left[\left| \frac{\partial^2 f_l}{\partial x^2} \right|^2 + 2 \left| \frac{\partial^2 f_l}{\partial x \partial y} \right|^2 + \left| \frac{\partial^2 f_l}{\partial y^2} \right|^2 \right] dx dy, \end{aligned}$$

where f_l is the restriction of f to \mathcal{T}_l as defined in (7). To construct the matrix \mathbf{Q} in Section III-B, we need a quadratic

form expression

$$\mathbf{c}_\ell^T \mathbf{Q}_\ell \mathbf{c}_\ell := \iint_{\mathcal{T}_\ell} \left[\left| \frac{\partial^2 f_\ell}{\partial x^2} \right|^2 + 2 \left| \frac{\partial^2 f_\ell}{\partial x \partial y} \right|^2 + \left| \frac{\partial^2 f_\ell}{\partial y^2} \right|^2 \right] dx dy, \quad (33)$$

where \mathbf{c}_ℓ is the B-coefficient vector of f_ℓ ($\ell = 1, 2, \dots, N$). Such an expression is found in [59] as summarized below.

Fact 4 ([59]): Let \mathcal{T}_ℓ be a triangle on \mathbb{R}^2 and $f_\ell : \mathcal{T}_\ell \rightarrow \mathbb{R}$ be a bivariate polynomial of degree $d \geq 2$ expressed as

$$f_\ell(x, y) = \sum_{i=0}^d \sum_{j=0}^i c_{\frac{i(i+1)}{2}+j+1} \frac{d!}{(d-i)!(i-j)!j!} r^{d-i} s^{i-j} t^j$$

by using its B-coefficients $\mathbf{c}_\ell := (c_1, c_2, \dots, c_{(d+1)(d+2)/2})^T$ and barycentric coordinate (r, s, t) of $(x, y) \in \mathcal{T}_\ell$ with respect to \mathcal{T}_ℓ . Then the symmetric positive semidefinite matrix $\mathbf{Q}_\ell \in \mathbb{R}^{\frac{(d+1)(d+2)}{2} \times \frac{(d+1)(d+2)}{2}}$ in (33) is given by

$$[\mathbf{Q}_\ell]_{\frac{i(i+1)}{2}+j+1, \frac{k(k+1)}{2}+l+1} := d^2(d-1)^2 \iint_{\mathcal{T}_\ell} e_{i,j,k,l}^{(d)} dx dy$$

for $0 \leq j \leq i \leq d$ and $0 \leq l \leq k \leq d$. Here $e_{i,j,k,l}^{(\zeta)} \in \mathbb{R}[r, s, t]$ ($2 \leq \zeta \leq d$, $0 \leq j \leq i \leq \zeta$ and $0 \leq l \leq k \leq \zeta$) are polynomials generated recursively from $e_{i,j,k,l}^{(2)}$ defined in (34) with $\mathbf{r} := (\frac{\partial r}{\partial x}, \frac{\partial r}{\partial y})^T$, $\mathbf{s} := (\frac{\partial s}{\partial x}, \frac{\partial s}{\partial y})^T$ and $\mathbf{t} := (\frac{\partial t}{\partial x}, \frac{\partial t}{\partial y})^T$, and

$$\begin{aligned} e_{i,j,k,l}^{(\zeta)} &:= r^2 e_{i,j,k-1,l}^{(\zeta-1)} + rs \left(e_{i,j,k-1,l}^{(\zeta-1)} + e_{i-1,j,k,l}^{(\zeta-1)} \right) \\ &+ rt \left(e_{i,j,k-1,l-1}^{(\zeta-1)} + e_{i-1,j-1,k,l}^{(\zeta-1)} \right) + s^2 e_{i-1,j,k-1,l}^{(\zeta-1)} \\ &+ st \left(e_{i-1,j,k-1,l-1}^{(\zeta-1)} + e_{i-1,j-1,k-1,l}^{(\zeta-1)} \right) + t^2 e_{i-1,j-1,k-1,l-1}^{(\zeta-1)} \end{aligned}$$

for $\zeta \geq 3$ (Note: $e_{i,j,k,l}^{(\zeta)} = 0$ if $i \notin [0, \zeta]$, $j \notin [0, i]$, $k \notin [0, \zeta]$, or $l \notin [0, k]$). \square

By combining Fact 4 with Fact 5 below, we can compute all components of \mathbf{Q}_ℓ ($\ell = 1, 2, \dots, N$) in closed form, from which, \mathbf{Q} in Section III-B is obtained.

Fact 5 ([46]): Let $\mathcal{T} := \langle \mathbf{v}_1, \mathbf{v}_2, \mathbf{v}_3 \rangle$ s.t. $\mathbf{v}_k := (x_k, y_k) \in \mathbb{R}^2$ ($k = 1, 2, 3$) and let (r, s, t) be barycentric coordinate of (x, y) with respect to \mathcal{T} . Then for any $(l, m, n) \in \mathbb{Z}_+^3$, we have

$$\iint_{\mathcal{T}} r^l s^m t^n dx dy = \frac{l!m!n!|\varrho|}{(d+2)!},$$

where $d := l + m + n$ and $\varrho := x_1 y_2 - y_1 x_2 + x_2 y_3 - y_2 x_3 + x_3 y_1 - y_3 x_1$. \square

APPENDIX D

FAST AND NUMERICALLY STABLE COMPUTATION FOR ALGEBRAIC PHASE UNWRAPPING WITH SUBRESULTANT

Suppose that univariate real polynomials

$$\left. \begin{aligned} \Psi_0(\tau) &= a_m \tau^m + a_{m-1} \tau^{m-1} + \dots + a_1 \tau + a_0 \\ \Psi_1(\tau) &= b_n \tau^n + b_{n-1} \tau^{n-1} + \dots + b_1 \tau + b_0 \end{aligned} \right\} \quad (35)$$

are given in Fact 3 and Fig. 2, where $a_m \neq 0$ and $b_n \neq 0$, i.e., $\deg(\Psi_0) = m$ and $\deg(\Psi_1) = n$ (Note: From (18), m and n are at most d in the scenario of Section III-C). Then for $l = 0, 1, \dots, \min\{m-1, n-1\}$, the l th *subresultant* $\text{Sres}_l[\Psi_0, \Psi_1](\tau) \in \mathbb{R}[\tau]$ of (Ψ_0, Ψ_1) is defined, as a univariate polynomial of degree l at most, by

$$\text{Sres}_l[\Psi_0, \Psi_1](\tau) := \begin{vmatrix} a_m \cdots a_{l+1} & a_l & \cdots & a_1 & a_0 & & \Psi_0(\tau)\tau^{n-l-1} \\ \vdots & \ddots & \ddots & & \ddots & \ddots & \vdots \\ & a_m & \cdots & a_{l+1} & a_l & \cdots & a_1 & a_0 & \Psi_0(\tau)\tau^{l+1} \\ & & a_m & \cdots & a_{l+1} & a_l & \cdots & a_1 & \Psi_0(\tau)\tau^l \\ & & & \ddots & \ddots & \ddots & \vdots & \vdots & \vdots \\ & & & & a_m & \cdots & a_{l+1} & a_l & \Psi_0(\tau)\tau \\ & & & & & a_m & \cdots & a_{l+1} & \Psi_0(\tau) \\ b_n \cdots b_{l+1} & b_l & \cdots & b_1 & b_0 & & \Psi_1(\tau)\tau^{m-l-1} \\ \vdots & \ddots & \ddots & & \ddots & \ddots & \vdots & \vdots & \vdots \\ & b_n & \cdots & b_{l+1} & b_l & \cdots & b_1 & b_0 & \Psi_1(\tau)\tau^{l+1} \\ & & b_n & \cdots & b_{l+1} & b_l & \cdots & b_1 & \Psi_1(\tau)\tau^l \\ & & & \ddots & \ddots & \ddots & \vdots & \vdots & \vdots \\ & & & & b_n & \cdots & b_{l+1} & b_l & \Psi_1(\tau)\tau \\ & & & & & b_n & \cdots & b_{l+1} & \Psi_1(\tau) \end{vmatrix}, \quad (36)$$

where $|\cdot|$ stands for the determinant of a matrix. In particular, $\text{Sres}_0[\Psi_0, \Psi_1] \in \mathbb{R}$ is called the *resultant* of (Ψ_0, Ψ_1) .

From the definitions of $V(\Psi(\tau^*))$ and $V(\Psi(a))$ (see Fact 3), for evaluating $V(\Psi(\tau^*))$ and $V(\Psi(a))$ in (19), we need only $\text{sgn}(\Psi_j(\tau^*))$ and $\text{sgn}(\Psi_j(a))$ ($j = 0, 1, \dots, q$) which can be computed by using $\text{Sres}_l[\Psi_0, \Psi_1](\tau^*)$ and $\text{Sres}_l[\Psi_0, \Psi_1](a)$ respectively as shown below.

Fact 6 (See [41, Theorem 4] for More General Cases): Let $(\Psi_j(\tau))_{j=0}^q$ be the polynomial sequence generated by the algorithm in Fig. 2, where $\Psi_0(\tau)$ and $\Psi_1(\tau)$ are given in (35). If $m \geq n$ and $\deg(\text{Sres}_l[\Psi_0, \Psi_1]) = l$ for all $l \in [0, n-1]$,

$$\left. \begin{aligned} e_{0,0,0,0}^{(2)} &= (\mathbf{r}^T \mathbf{r})^2; & e_{1,0,1,1}^{(2)} &= e_{1,1,1,0}^{(2)} = 2\mathbf{r}^T \mathbf{r} \mathbf{s}^T \mathbf{t} + 2\mathbf{r}^T \mathbf{s} \mathbf{r}^T \mathbf{t}; & e_{1,1,2,2}^{(2)} &= e_{2,2,1,1}^{(2)} = 2\mathbf{t}^T \mathbf{t} \mathbf{t}^T \mathbf{r} \\ e_{0,0,1,0}^{(2)} &= e_{1,0,0,0}^{(2)} = 2\mathbf{r}^T \mathbf{r} \mathbf{r}^T \mathbf{s}; & e_{1,0,2,0}^{(2)} &= e_{2,0,1,0}^{(2)} = 2\mathbf{s}^T \mathbf{s} \mathbf{s}^T \mathbf{r}; & e_{2,0,2,0}^{(2)} &= (\mathbf{s}^T \mathbf{s})^2 \\ e_{0,0,1,1}^{(2)} &= e_{1,1,0,0}^{(2)} = 2\mathbf{r}^T \mathbf{r} \mathbf{r}^T \mathbf{t}; & e_{1,0,2,1}^{(2)} &= e_{2,1,1,0}^{(2)} = 2\mathbf{s}^T \mathbf{s} \mathbf{r}^T \mathbf{t} + 2\mathbf{s}^T \mathbf{r} \mathbf{s}^T \mathbf{t}; & e_{2,0,2,1}^{(2)} &= e_{2,1,2,0}^{(2)} = 2\mathbf{s}^T \mathbf{s} \mathbf{s}^T \mathbf{t} \\ e_{0,0,2,0}^{(2)} &= e_{2,0,0,0}^{(2)} = (\mathbf{r}^T \mathbf{s})^2; & e_{1,0,2,2}^{(2)} &= e_{2,2,1,0}^{(2)} = 2\mathbf{t}^T \mathbf{r} \mathbf{t}^T \mathbf{s}; & e_{2,0,2,2}^{(2)} &= e_{2,2,2,0}^{(2)} = (\mathbf{s}^T \mathbf{t})^2 \\ e_{0,0,2,1}^{(2)} &= e_{2,1,0,0}^{(2)} = 2\mathbf{r}^T \mathbf{s} \mathbf{r}^T \mathbf{t}; & e_{1,1,1,1}^{(2)} &= 2\mathbf{r}^T \mathbf{r} \mathbf{t}^T \mathbf{t} + 2(\mathbf{r}^T \mathbf{t})^2; & e_{2,1,2,1}^{(2)} &= 2\mathbf{s}^T \mathbf{s} \mathbf{t}^T \mathbf{t} + 2(\mathbf{s}^T \mathbf{t})^2 \\ e_{0,0,2,2}^{(2)} &= e_{2,2,0,0}^{(2)} = (\mathbf{r}^T \mathbf{t})^2; & e_{1,1,2,0}^{(2)} &= e_{2,0,1,1}^{(2)} = 2\mathbf{s}^T \mathbf{r} \mathbf{s}^T \mathbf{t}; & e_{2,1,2,2}^{(2)} &= e_{2,2,2,1}^{(2)} = 2\mathbf{t}^T \mathbf{t} \mathbf{t}^T \mathbf{s} \\ e_{1,0,1,0}^{(2)} &= 2\mathbf{r}^T \mathbf{r} \mathbf{s}^T \mathbf{s} + 2(\mathbf{r}^T \mathbf{s})^2; & e_{1,1,2,1}^{(2)} &= e_{2,1,1,1}^{(2)} = 2\mathbf{t}^T \mathbf{t} \mathbf{r}^T \mathbf{s} + 2\mathbf{t}^T \mathbf{r} \mathbf{t}^T \mathbf{s}; & e_{2,2,2,2}^{(2)} &= (\mathbf{t}^T \mathbf{t})^2 \end{aligned} \right\} \quad (34)$$

then we have $q = n + 1$ and

$$\begin{aligned} \text{sgn}(\Psi_j(\tau)) &= (-1)^{(j-1)j/2+(j-1)(m-n+1)} \\ &\quad \cdot \text{sgn}(b_n^{m-n+1} \text{Sres}_{n-j+1}[\Psi_0, \Psi_1](\tau)) \end{aligned}$$

for $j = 2, 3, \dots, n + 1$. \square

Note that computation of $\text{Sres}_j[\Psi_0, \Psi_1](\tau)$ in (36) does not require any polynomial division, which results in stable computation of $V(\Psi(\tau^*))$ and $V(\Psi(a))$. If we are interested in $\{\theta_{f^*}(\mathbf{v}_2^{(K)})\}_{K=1}^N$ (see Section III-C), the expressions in (17), (18) and (19) indicate that only $\text{Sres}_{n-j+1}[\Psi_0, \Psi_1](0)$ and $\text{Sres}_{n-j+1}[\Psi_0, \Psi_1](1)$ ($j = 2, 3, \dots, n + 1$) are necessary to obtain $V(\Psi(0))$ and $V(\Psi(1))$ for given polynomials $P_{(k)}(\tau) := F_{(k)}^{(i)}(\tau) \in \mathbb{R}[\tau]$ ($k = 0, 1$ and $i = 1, 2, \dots, K$). Moreover, for any $\Psi_k(\tau) \in \mathbb{R}[\tau]$ ($k = 0, 1$) in (35),⁹ the expression in (36) indicates that $\text{Sres}_{n-j+1}[\Psi_0, \Psi_1](0)$ and $\text{Sres}_{n-j+1}[\Psi_0, \Psi_1](1)$ can be expressed as multivariate polynomials of coefficients of $\Psi_0(\tau)$ and $\Psi_1(\tau)$, where the total degrees of $\text{Sres}_{n-j+1}[\Psi_0, \Psi_1](0) \in \mathbb{R}[a_0, \dots, a_m, b_0, \dots, b_n]$ and $\text{Sres}_{n-j+1}[\Psi_0, \Psi_1](1) \in \mathbb{R}[a_0, \dots, a_m, b_0, \dots, b_n]$ are $(m - n + 2j - 2)$. Since these multivariate polynomials can be constructed beforehand, fast and stable evaluations of $V(\Psi(0))$ and $V(\Psi(1))$ are realized by substituting each coefficient of $\Psi_0(\tau)$ and $\Psi_1(\tau)$ to the multivariate polynomials.

APPENDIX E

DERIVATIONS OF RELATIONS (26) AND (28)

Consider the unwrapped phase $\Theta := \Theta_{\text{int}} - \Theta_{\text{ref}}$ as a bivariate function defined for $(R_1, H) \in \mathbb{R}_{++} \times \mathbb{R}_+$ not for $(x, y) \in \Omega$. By letting $\Theta_{\text{ref}}(R_1) := \Theta_{\text{int}}(R_1, H_0)$ and $\Theta(R_1, H) := \Theta_{\text{int}}(R_1, H) - \Theta_{\text{ref}}(R_1)$, we have $\Theta(R_1, H_0) = 0$ for all R_1 , and can verify from (24), with some algebra,

$$\frac{\partial \Theta}{\partial H} = \frac{\partial \Theta_{\text{int}}}{\partial H} = \frac{4\pi R_1 B \cos(\theta_o - \alpha)}{\lambda \sqrt{R_1^2 + B^2 - 2R_1 B \sin(\theta_o - \alpha)}} \cdot \frac{\partial \theta_o}{\partial H}. \quad (37)$$

Moreover, from $\theta_o = \arccos\left(\frac{R_1^2 + (R_E + H_{\text{SAR}})^2 - (R_E + H)^2}{2R_1(R_E + H_{\text{SAR}})}\right)$,¹⁰ we have

$$\begin{aligned} \frac{\partial \theta_o}{\partial H} &= \left(-\frac{1}{\sin \theta_o}\right) \cdot \left(-\frac{R_E + H}{R_1(R_E + H_{\text{SAR}})}\right) \\ &= \frac{1}{R_1} \cdot \frac{R_E + H}{(R_E + H_{\text{SAR}}) \sin \theta_o} = \frac{1}{R_1 \sin \theta_i}. \quad (38) \end{aligned}$$

Then, from (37) and (38), we derive (26):

$$\begin{aligned} \frac{\partial \Theta}{\partial H} &= \frac{\partial \Theta_{\text{int}}}{\partial H} \\ &= \frac{4\pi B \cos(\theta_o(R_1, H) - \alpha)}{\lambda \sin \theta_i(R_1, H) \sqrt{R_1^2 + B^2 - 2R_1 B \sin(\theta_o(R_1, H) - \alpha)}}, \end{aligned}$$

where the dependencies of θ_o and θ_i on (R_1, H) are clearly expressed. These relations show that the unwrapped phase Θ

⁹For any $P_{(k)}(\tau) := F_{(k)}^{(i)}(\tau) \in \mathbb{R}[\tau]$ ($k = 0, 1$ and $i = 1, 2, \dots, K$), $\Psi_k(\tau) := P_{(k)}(\tau)/\tau^{e_k}$ ($k = 0, 1$ and e_k is the order of $\tau = 0$ as a zero of $P_{(k)}(\tau)$) can be computed precisely in digital computer because the evaluation of $P_{(k)}(0)$ and the polynomial division of $P_{(k)}(\tau)$ by τ are implemented without any numerical errors.

¹⁰ $\arccos : \mathbb{R} \rightarrow [0, \pi]$ returns the principal value of the inverse cosine, i.e., $\cos(\arccos(x)) = x$ for all $x \in [-1, 1]$.

at any (R_1^*, H^*) can be expressed as shown in (28):

$$\begin{aligned} \Theta(R_1^*, H^*) &= \Theta(R_1^*, H_0) + \int_{H_0}^{H^*} \frac{\partial \Theta}{\partial H} \Big|_{R_1=R_1^*} dH \\ &= \int_{H_0}^{H^*} \frac{4\pi B \cos(\theta_o^H - \alpha)}{\lambda \sin \theta_i^H \sqrt{R_1^{*2} + B^2 - 2R_1^* B \sin(\theta_o^H - \alpha)}} dH \\ &\approx \int_{H_0}^{H^*} \frac{4\pi B \cos(\theta_o^{H_0} - \alpha)}{\lambda \sin \theta_i^{H_0} \sqrt{R_1^{*2} + B^2 - 2R_1^* B \sin(\theta_o^{H_0} - \alpha)}} dH \\ &= \frac{4\pi B \cos(\theta_o^{H_0} - \alpha)}{\lambda \sin \theta_i^{H_0} \sqrt{R_1^{*2} + B^2 - 2R_1^* B \sin(\theta_o^{H_0} - \alpha)}} (H^* - H_0), \end{aligned}$$

where $\theta_o^H := \theta_o(R_1^*, H)$ and $\theta_i^H := \theta_i(R_1^*, H)$. The above approximation is justified from the fact that θ_o^H and θ_i^H change very slowly if R_1 and H_{SAR} are sufficiently large compared with $(H^* - H_0)$.

Note that, under the assumption $0 < x := \frac{B}{R_1} \ll 1$, Θ_{int} in (24) can be approximated as

$$\Theta_{\text{int}} \approx \frac{4\pi B \sin(\theta_o - \alpha)}{\lambda} =: \hat{\Theta}_{\text{int}} \quad (39)$$

with the use of the *first order Taylor series approximation* of $\sqrt{1 + x^2 - 2x \sin(\theta_o - \alpha)} \approx 1 - x \sin(\theta_o - \alpha)$. Finally, by using (39), we derive

$$\frac{\partial \Theta}{\partial H} \approx \frac{\partial \hat{\Theta}_{\text{int}}}{\partial H} = \frac{4\pi B \cos(\theta_o - \alpha)}{\lambda} \cdot \frac{\partial \theta_o}{\partial H} = \frac{4\pi B \cos(\theta_o - \alpha)}{\lambda R_1 \sin \theta_i},$$

which is (27), and

$$\begin{aligned} \Theta(R_1^*, H^*) &= \Theta(R_1^*, H_0) + \int_{H_0}^{H^*} \frac{\partial \Theta}{\partial H} \Big|_{R_1=R_1^*} dH \\ &\approx \int_{H_0}^{H^*} \frac{4\pi B \cos(\theta_o^H - \alpha)}{\lambda R_1^* \sin \theta_i^H} dH \\ &\approx \int_{H_0}^{H^*} \frac{4\pi B \cos(\theta_o^{H_0} - \alpha)}{\lambda R_1^* \sin \theta_i^{H_0}} dH \\ &= \frac{4\pi B \cos(\theta_o^{H_0} - \alpha)}{\lambda R_1^* \sin \theta_i^{H_0}} (H^* - H_0), \end{aligned}$$

which is found, e.g., in [80, Equation (A.2.7)].¹¹

ACKNOWLEDGMENT

The authors would like to thank the anonymous reviewers for their many constructive comments which were very helpful to improve the readability of this paper, in particular, Section III-D. They also thank Dr. Masao Yamagishi of the Tokyo Institute of Technology for fruitful discussion.

REFERENCES

- [1] D. C. Ghiglia and M. D. Pritt, *Two-Dimensional Phase Unwrapping: Theory, Algorithms, and Software*. New York, NY: Wiley, 1998.
- [2] L. Ying, "Phase unwrapping," in *Wiley Encyclopedia of Biomedical Engineering, 6-Volume Set*, M. Akay, Ed. New York, NY: Wiley, 2006.
- [3] L. C. Graham, "Synthetic interferometer radar for topographic mapping," *Proceedings of the IEEE*, vol. 62, no. 6, pp. 763–768, Jun. 1974.

¹¹In [80, Equation (A.2.7)], the variables $\Delta\phi$, R , B_n , q , θ , and d correspond to $-\Theta$, R_1 , $B \cos(\theta_o^{H_0} - \alpha)$, $H - H_0$, $\theta_i^{H_0}$, and 0, respectively, in this paper.

- [4] H. A. Zebker and R. M. Goldstein, "Topographic mapping from interferometric synthetic aperture radar observations," *Journal of Geophysical Research*, vol. 91, no. B5, pp. 4993–4999, Apr. 1986.
- [5] R. M. Goldstein, H. A. Zebker, and C. L. Werner, "Satellite radar interferometry: Two-dimensional phase unwrapping," *Radio Science*, vol. 23, no. 4, pp. 713–720, Jul./Aug. 1988.
- [6] A. Moccia and S. Vetralla, "A tethered interferometric synthetic aperture radar (SAR) for a topographic mission," *IEEE Transactions on Geoscience and Remote Sensing*, vol. 30, no. 1, pp. 103–109, Jan. 1992.
- [7] P. A. Rosen, S. Hensley, I. R. Joughin, F. K. Li, S. N. Madsen, E. Rodriguez, and R. M. Goldstein, "Synthetic aperture radar interferometry," *Proceedings of the IEEE*, vol. 88, no. 3, pp. 333–382, Mar. 2000.
- [8] D. Leva, G. Nico, D. Tarchi, J. Fortuny, and A. J. Sieber, "Temporal analysis of a landslide by means of a ground-based SAR interferometer," *IEEE Transactions on Geoscience and Remote Sensing*, vol. 4, no. 4, pp. 745–752, Apr. 2003.
- [9] C. Colesanti and J. Wasowski, "Investigating landslides with space-borne synthetic aperture radar (SAR) interferometry," *Engineering Geology*, vol. 88, no. 3–4, pp. 173–199, Dec. 2006.
- [10] C. de Moustier and H. Matsumoto, "Seafloor acoustic remote sensing with multibeam echo-sounders and bathymetric sidescan sonar systems," *Marine Geophysical Researches*, vol. 15, no. 1, pp. 27–42, Jan. 1993.
- [11] P. N. Denbigh, "Signal processing strategies for a bathymetric sidescan sonar," *IEEE Journal of Oceanic Engineering*, vol. 19, no. 3, pp. 382–390, Jul. 1994.
- [12] R. E. Hansen, T. O. Sæbø, K. Gade, and S. Chapman, "Signal processing for AUV based interferometric synthetic aperture sonar," in *Proceedings of MTS/IEEE OCEANS*, 2003, vol. 5, pp. 2438–2444.
- [13] M. P. Hayes and P. T. Gough, "Synthetic aperture sonar: A review of current status," *IEEE Journal of Oceanic Engineering*, vol. 34, no. 3, pp. 207–224, Jul. 2009.
- [14] V. Srinivasan, H. C. Liu, and M. Halioua, "Automated phase-measuring profilometry: A phase mapping approach," *Applied Optics*, vol. 24, no. 2, pp. 185–188, Jan. 1985.
- [15] H. Zhao, W. Chen, and Y. Tan, "Phase-unwrapping algorithm for the measurement of three-dimensional object shapes," *Applied Optics*, vol. 33, no. 20, pp. 4497–4500, Jul. 1994.
- [16] P. S. Huang, C. Zhang, and F. P. Chiang, "High-speed 3-D shape measurement based on digital fringe projection," *Optical Engineering*, vol. 42, no. 1, pp. 163–168, Jan. 2003.
- [17] S. Zhang, "Recent progresses on real-time 3D shape measurement using digital fringe projection techniques," *Optics and Lasers in Engineering*, vol. 48, no. 2, pp. 149–158, Feb. 2010.
- [18] P. Cloetens, W. Ludwig, J. Baruchel, D. Van Dyck, J. Van Landuyt, J. P. Guigay, and M. Schlenker, "Holotomography: Quantitative phase tomography with micrometer resolution using hard synchrotron radiation x rays," *Applied Physics Letters*, vol. 75, no. 19, pp. 2912–2914, Nov. 1999.
- [19] T. Weitkamp, A. Diaz, C. David, F. Pfeiffer, M. Stampanoni, P. Cloetens, and E. Ziegler, "X-ray phase imaging with a grating interferometer," *Optics Express*, vol. 13, no. 16, pp. 6296–6304, Aug. 2005.
- [20] A. Momose, W. Yashiro, Y. Takeda, Y. Suzuki, and T. Hattori, "Phase tomography by X-ray Talbot interferometry for biological imaging," *Japanese Journal of Applied Physics*, vol. 45, no. 6A, pp. 5254–5262, Jun. 2006.
- [21] M. Dierolf, A. Menzel, P. Thibault, P. Schneider, C. M. Kewish, R. Wepf, O. Bunk, and F. Pfeiffer, "Ptychographic X-ray computed tomography at the nanoscale," *Nature*, vol. 467, no. 7314, pp. 436–439, Sep. 2010.
- [22] G. H. Glover and E. Schneider, "Three-point Dixon technique for true water/fat decomposition with B_0 inhomogeneity correction," *Magnetic Resonance in Medicine*, vol. 18, no. 2, pp. 371–383, Apr. 1991.
- [23] J. Szumowski, W. R. Coshov, F. Li, and S. F. Quinn, "Phase unwrapping in the three-point Dixon method for fat suppression MR imaging," *Radiology*, vol. 192, no. 2, pp. 555–561, Aug. 1994.
- [24] S. M. Song, S. Napel, N. J. Pelc, and G. H. Glover, "Phase unwrapping of MR phase images using Poisson equation," *IEEE Transactions on Image Processing*, vol. 4, no. 5, pp. 667–676, May 1995.
- [25] S. Chaves, Q. S. Xiang, and L. An, "Understanding phase maps in MRI: A new outline phase unwrapping method," *IEEE Transactions on Medical Imaging*, vol. 21, no. 8, pp. 966–977, Aug. 2002.
- [26] C. W. Chen and H. A. Zebker, "Network approaches to two-dimensional phase unwrapping: Intractability and two new algorithms," *Journal of the Optical Society of America A: Optics, Image Science, and Vision*, vol. 17, no. 3, pp. 401–414, Mar. 2000.
- [27] J. R. Buckland, J. M. Huntley, and S. R. E. Turner, "Unwrapping noisy phase maps by use of a minimum cost matching algorithm," *Applied Optics*, vol. 34, no. 23, pp. 5100–5108, Aug. 1995.
- [28] T. J. Flynn, "Two-dimensional phase unwrapping with minimum weighted discontinuity," *Journal of the Optical Society of America A: Optics, Image Science, and Vision*, vol. 14, no. 10, pp. 2692–2701, Oct. 1997.
- [29] M. Costantini, "A novel phase unwrapping method based on network programming," *IEEE Transactions on Geoscience and Remote Sensing*, vol. 36, no. 3, pp. 813–821, May 1998.
- [30] C. W. Chen and H. A. Zebker, "Two-dimensional phase unwrapping with use of statistical models for cost functions in nonlinear optimization," *Journal of the Optical Society of America A: Optics, Image Science, and Vision*, vol. 18, no. 2, pp. 338–351, Feb. 2001.
- [31] H. Takajo and T. Takahashi, "Least-squares phase estimation from the phase difference," *Journal of the Optical Society of America A: Optics, Image Science, and Vision*, vol. 5, no. 3, pp. 416–425, Jan. 1988.
- [32] D. C. Ghiglia and L. A. Romero, "Robust two-dimensional weighted and unweighted phase unwrapping that uses fast transforms and iterative methods," *Journal of the Optical Society of America A: Optics, Image Science, and Vision*, vol. 11, no. 1, pp. 107–117, Jan. 1994.
- [33] M. D. Pritt and J. S. Shipman, "Least-squares two-dimensional phase unwrapping using FFTs," *IEEE Transactions on Geoscience and Remote Sensing*, vol. 32, no. 3, pp. 706–708, May 1994.
- [34] D. C. Ghiglia and L. A. Romero, "Minimum L^p -norm two-dimensional phase unwrapping," *Journal of the Optical Society of America A: Optics, Image Science, and Vision*, vol. 13, no. 10, pp. 1999–2013, Oct. 1996.
- [35] B. W. Silverman, "Some aspects of the spline smoothing approach to non-parametric regression curve fitting," *Journal of the Royal Statistical Society: Series B (Statistical Methodology)*, vol. 47, no. 1, pp. 1–52, 1985.
- [36] G. Wahba, *Spline Models for Observational Data*, ser. CBMS-NSF Regional Conference Series in Applied Mathematics. Philadelphia, PA: SIAM, 1990, vol. 59.
- [37] J. O. Ramsay and B. W. Silverman, *Functional Data Analysis*, 2nd ed. New York, NY: Springer, 2005.
- [38] I. Yamada, K. Kurosawa, H. Hasegawa, and K. Sakaniwa, "Algebraic multidimensional phase unwrapping and zero distribution of complex polynomials—Characterization of multivariate stable polynomials," *IEEE Transactions on Signal Processing*, vol. 46, no. 6, pp. 1639–1664, Jun. 1998.
- [39] I. Yamada and N. K. Bose, "Algebraic phase unwrapping and zero distribution of polynomial for continuous-time systems," *IEEE Transactions on Circuits and Systems—Part I: Fundamental Theory and Applications*, vol. 49, no. 3, pp. 298–304, Mar. 2002.
- [40] I. Yamada and K. Oguchi, "High-resolution estimation of the directions-of-arrival distribution by algebraic phase unwrapping algorithms," *Multidimensional Systems and Signal Processing*, vol. 22, no. 1–3, pp. 191–211, Mar. 2011.
- [41] D. Kitahara and I. Yamada, "Algebraic phase unwrapping along the real axis: Extensions and stabilizations," *Multidimensional Systems and Signal Processing*, vol. 26, no. 1, pp. 3–45, Jan. 2015.
- [42] D. Kitahara and I. Yamada, "Algebraic phase unwrapping for functional data analytic estimations—Extensions and stabilizations," in *Proceedings of IEEE International Conference on Acoustics, Speech and Signal Processing (ICASSP)*, 2013, pp. 5835–5839.
- [43] H. A. Zebker and Y. Lu, "Phase unwrapping algorithms for radar interferometry: Residue-cut, least-squares, and synthesis algorithms," *Journal of the Optical Society of America A: Optics, Image Science, and Vision*, vol. 15, no. 3, pp. 586–598, Mar. 1998.
- [44] H. Braunisch, B. Wu, and J. A. Kong, "Phase unwrapping of SAR interferograms after wavelet denoising," in *Proceedings of IEEE International Geoscience and Remote Sensing Symposium (IGARSS)*, 2000, vol. 2, pp. 752–754.
- [45] A. Suksmono and A. Hirose, "Adaptive noise reduction of InSAR images based on a complex-valued MRF model and its application to phase unwrapping problem," *IEEE Transactions on Geoscience and Remote Sensing*, vol. 40, no. 3, pp. 699–709, Mar. 2002.
- [46] C. K. Chui and M. J. Lai, "Multivariate vertex splines and finite elements," *Journal of Approximation Theory*, vol. 60, no. 3, pp. 245–343, Mar. 1990.
- [47] G. Farin, "Triangular Bernstein-Bézier patches," *Computer Aided Geometric Design*, vol. 3, no. 2, pp. 83–127, Aug. 1986.
- [48] M. J. Lai, "Geometric interpretation of smoothness conditions of triangular polynomial patches," *Computer Aided Geometric Design*, vol. 14, no. 2, pp. 191–199, Feb. 1997.
- [49] C. K. Chui, *Multivariate Splines*, ser. CBMS-NSF Regional Conference Series in Applied Mathematics. Philadelphia, PA: SIAM, 1988, vol. 54.
- [50] G. E. Fasshauer and L. L. Schumaker, "Minimal energy surfaces using parametric splines," *Computer Aided Geometric Design*, vol. 13, no. 1, pp. 45–79, Feb. 1996.

- [51] M. J. Lai and L. L. Schumaker, *Spline Functions on Triangulations*. New York, NY: Cambridge University Press, 2007.
- [52] M. J. Lai, "Multivariate splines and their applications," in *Computational Complexity: Theory, Techniques, and Applications*, R. A. Meyers, Ed. New York, NY: Springer, 2012, pp. 1939–1980.
- [53] A. Galbis and M. Maestre, *Vector Analysis Versus Vector Calculus*. New York, NY: Springer, 2012.
- [54] C. de Boor, "Best approximation properties of spline functions of odd degree," *Journal of Mathematics and Mechanics*, vol. 12, no. 5, pp. 747–749, 1963.
- [55] J. H. Ahlberg, E. N. Nilson, and J. L. Walsh, *The Theory of Splines and Their Applications*. New York, NY: Academic Press, 1967.
- [56] V. Pretlová, "Bicubic spline smoothing of two-dimensional geophysical data," *Studia Geophysica et Geodaetica*, vol. 20, no. 2, pp. 168–177, Jun. 1976.
- [57] E. J. Wegman and I. W. Wright, "Splines in statistics," *Journal of the American Statistical Association*, vol. 78, no. 382, pp. 351–365, Jan. 1983.
- [58] M. Unser, "Splines: A perfect fit for signal and image processing," *IEEE Signal Processing Magazine*, vol. 16, no. 6, pp. 22–38, Nov. 1999.
- [59] E. Quak and L. L. Schumaker, "Calculation of the energy of a piecewise polynomial surface," in *Algorithms for Approximation II*, M. G. Cox and J. C. Mason, Eds. London, UK: Chapman & Hall, 1990, pp. 134–143.
- [60] D. Goldfarb and S. Liu, "An $O(n^3L)$ primal interior point algorithm for convex quadratic programming," *Mathematical Programming*, vol. 49, no. 1, pp. 325–340, Nov. 1990.
- [61] Y. Nesterov and A. Nemirovskii, *Interior-Point Polynomial Algorithms in Convex Programming*, ser. Studies in Applied and Numerical Mathematics. Philadelphia, PA: SIAM, 1994, vol. 13.
- [62] J. Nocedal and S. J. Wright, *Numerical Optimization*, 2nd ed., ser. Operations Research and Financial Engineering. New York, NY: Springer, 2006.
- [63] I. Yamada, "The hybrid steepest descent method for the variational inequality problem over the intersection of fixed point sets of non-expansive mappings," in *Inherently Parallel Algorithms in Feasibility and Optimization and their Applications*, ser. Studies in Computational Mathematics, D. Butnariu, Y. Censor, and S. Reich, Eds. Amsterdam, The Netherlands: Elsevier, 2001, vol. 8, pp. 473–504.
- [64] I. Yamada, N. Ogura, and N. Shirakawa, "A numerically robust hybrid steepest descent method for the convexly constrained generalized inverse problems," in *Inverse Problems, Image Analysis, and Medical Imaging*, ser. Contemporary Mathematics, M. Z. Nashed and O. Scherzer, Eds. Providence, RI: American Mathematical Society, 2002, vol. 313, pp. 269–305.
- [65] N. Ogura and I. Yamada, "Nonstrictly convex minimization over the bounded fixed point set of a nonexpansive mapping," *Numerical Functional Analysis and Optimization*, vol. 24, no. 1–2, pp. 129–135, 2003.
- [66] I. Yamada and N. Ogura, "Hybrid steepest descent method for variational inequality problem over the fixed point sets of certain quasi-nonexpansive mappings," *Numerical Functional Analysis and Optimization*, vol. 25, no. 7–8, pp. 619–655, 2005.
- [67] I. Yamada, M. Yukawa, and M. Yamagishi, "Minimizing the moreau envelope of nonsmooth convex functions over the fixed point set of certain quasi-nonexpansive mappings," in *Fixed-Point Algorithms for Inverse Problems in Science and Engineering*, H. H. Bauschke, R. S. Burachik, P. L. Combettes, V. Elser, D. R. Luke, and H. Wolkowicz, Eds. New York, NY: Springer, 2011, pp. 345–390.
- [68] S. Ono and I. Yamada, "Hierarchical convex optimization with primal-dual splitting," *IEEE Transactions on Signal Processing*, vol. 2, no. 63, pp. 373–388, Jan. 2015.
- [69] W. S. Brown and J. F. Traub, "On Euclid's algorithm and the theory of subresultants," *Journal of the ACM*, vol. 18, no. 4, pp. 505–514, Oct. 1971.
- [70] C. K. Chui and R. H. Wang, "Multivariate spline spaces," *Journal of Mathematical Analysis and Applications*, vol. 94, no. 1, pp. 197–221, Jun. 1983.
- [71] B. Kampes, E. Steenbergen, and R. Hanssen, InSAR Matlab Toolbox ver. 1.1 [Online]. Available: http://doris.tudelft.nl/Doris_download.html
- [72] R. Bamler and P. Hartl, "Synthetic aperture radar interferometry," *Inverse Problems*, vol. 14, no. 4, pp. R1–R54, Aug. 1998.
- [73] R. F. Hanssen, *Radar Interferometry: Data Interpretation and Error Analysis*. Dordrecht, The Netherlands: Kluwer, 2001.
- [74] H. Bähr, *Orbital Effects in Spaceborne Synthetic Aperture Radar Interferometry*. Karlsruhe, Germany: KIT Scientific Publishing, 2013.
- [75] L. I. Rudin, S. Osher, and E. Fatemi, "Nonlinear total variation based noise removal algorithms," *Physica D: Nonlinear Phenomena*, vol. 60, no. 1–4, pp. 259–268, Nov. 1992.
- [76] C. R. Vogel and M. E. Oman, "Iterative methods for total variation denoising," *SIAM Journal on Scientific Computing*, vol. 17, no. 1, pp. 227–238, 1996.
- [77] D. Gabay and B. Mercier, "A dual algorithm for the solution of nonlinear variational problems via finite element approximation," *Computers & Mathematics with Applications*, vol. 2, no. 1, pp. 17–40, 1976.
- [78] M. Fortin and R. Glowinski, *Augmented Lagrangian Methods: Applications to the Numerical Solution of Boundary-Value Problems*, ser. Studies in Mathematics and Its Applications. Amsterdam, The Netherlands: Elsevier, 1983, vol. 15.
- [79] J. Eckstein and D. P. Bertsekas, "On the Douglas-Rachford splitting method and the proximal point algorithm for maximal monotone operators," *Mathematical Programming*, vol. 55, no. 1, pp. 293–318, Apr. 1992.
- [80] A. Ferretti, A. Monti-Guarnieri, C. Prati, F. Rocca, and D. Massonnet, *InSAR Principles: Guidelines for SAR Interferometry Processing and Interpretation*, K. Fletcher, Ed. Noordwijk, The Netherlands: ESA Publications, 2007, vol. TM-19.
- [81] R. K. Ahuja, T. L. Magnanti, and J. Orlin, *Network Flows: Theory, Algorithms, and Applications*. Englewood Cliffs, NJ: Prentice Hall, 1993.



Daichi Kitahara (S'13) received the B.E. degree in computer science and the M.E. degree in communications and computer engineering from the Tokyo Institute of Technology in 2012 and 2014, respectively. Since 2014, he has been a Ph.D. student in the Department of Communications and Computer Engineering, Tokyo Institute of Technology.

Since April 2014, he has been a recipient of the Research Fellowship of the Japan Society for the Promotion of Science (JSPS). His current research interests are in signal processing and its applications, inverse problem, optimization theory, and multivariate spline theory.

He received two Young Researcher Awards respectively from the IEICE Technical Group on Signal Processing in 2013 and from the SICE Technical Committee on Remote Sensing in 2015.



Isao Yamada (M'96–SM'06–F'15) received the B.E. degree in computer science from the University of Tsukuba in 1985 and the M.E. and the Ph.D. degrees in electrical and electronic engineering from the Tokyo Institute of Technology, Tokyo, Japan, in 1987 and 1990, respectively.

He is a Professor with the Department of Communications and Computer Engineering, and the Director of the GSIC (Global Scientific Information and Computing Center), Tokyo Institute of Technology. His current research interests are in mathematical signal processing, nonlinear inverse problem, and optimization theory.

Dr. Yamada has been an Associate Editor for several journals, including the *IEICE Transactions on Fundamentals of Electronics, Communications and Computer Sciences* (2001–2005), the *IEEE TRANSACTIONS ON CIRCUITS AND SYSTEMS—PART I: FUNDAMENTAL THEORY AND APPLICATIONS* (2006–2007), and the *IEEE TRANSACTIONS ON SIGNAL PROCESSING* (2008–2011). He also served as the Editor-in-Chief of the *IEICE Transactions on Fundamentals* (2013–2015). Currently, he is serving as an editorial board member of the *IEEE TRANSACTIONS ON SIGNAL AND INFORMATION PROCESSING OVER NETWORKS* (2014 to present), the *Numerical Functional Analysis and Optimization* (Taylor and Francis) and the *Multidimensional Systems and Signal Processing* (Springer).

He has been serving as a Steering Committee member of IEICE Engineering Sciences Society, including the Chairman of the IEICE Technical Group on Signal Processing in 2011 and the Vice President (System and Signal Processing) in 2012. He has also served as a member of the IEEE Signal Processing Theory and Methods Technical Committee (2009–2014). He received the 2014 IEEE Signal Processing Magazine Best Paper Award from the IEEE Signal Processing Society in 2015, the Excellent Paper Awards in 1991, 1995, 2006, 2009 and 2014, the Young Researcher Award in 1992, and the Achievement Award in 2009 from the IEICE; the ICF Research Award from the International Communications Foundation in 2004; the Docomo Mobile Science Award (Fundamental Science Division) from Mobile Communication Fund in 2005; and the Fujino Prize from Teijima Foundation in 2008. In 2015, he became the IEICE Fellow.